RSC Sustainability

ROYAL SOCIETY OF CHEMISTRY

CRITICAL REVIEW

View Article Online
View Journal | View Issue

Cite this: *RSC Sustainability*, 2024, **2**, 1224

Green supercapacitors: review and perspectives on sustainable template-free synthesis of metal and metal oxide nanoparticles

Jayaprakash Meena,[a] Shapna shankari Sivasubramaniam,[a] Ezhumalai David [b] and Santhakumar K *[a]

Researchers are committed to thoroughly investigating the sustainable production of supercapacitor electrode materials with enhanced properties. Supercapacitors are promising energy storage devices due to their high power density, stability, rapid energy storage, and fast delivery, but most materials employed for the fabrication of electrodes are toxic and not environmentally friendly. Thus, to overcome this issue, there has been considerable interest in green, eco-friendly, biocompatible, and biodegradable materials for use in various energy devices. Modified electrode materials are created through phytosynthesis, which have been proven to act as excellent reducing agents and improved catalysts, while maintaining a desirable shape and size, making them ideal for use as noble supercapacitor electrode materials. To fully realize the capabilities of using plant extracts to assemble nano-energy materials in different dimensions, it is important to have a thorough comprehension of the structure and properties of natural components and micro/nanostructures. This review provides an outline of the latest advancements in the design and construction of free-standing supercapacitor electrodes using plant-based materials. Initially, we emphasize the importance of green synthesis and phytosynthesis characteristics, including the factors affecting them and their plausible mechanisms. Further, we outline phytosynthesized nanomaterials and composites for supercapacitor applications with basic technology. We aim to systematically discuss the potential impact of greener methods using various plant-based synthesized metal nanoparticles (such as Ti, V, Cr, Mn, Ni, Fe, Co, Zn, Cu, Ni, W, Au, and Pt) for supercapacitor application and their conceivable mechanism. We conclude with a summary of the challenges for the future development of sustainable supercapacitor electrode materials.

Received 10th January 2024
Accepted 13th March 2024

DOI: 10.1039/d4su00009a

rsc.li/rscsus

Sustainability spotlight

This review provides an outline of the latest advancements in designing and constructing free-standing supercapacitor electrodes using plant-based materials. The benefits of using a greener approach over a conventional one have also been presented to get a green future with green energy technology. It is projected that phytosynthesized NPs will be one of the most promising materials in the future based on their preparation cost, electrical conductivity, cyclic stability performance, and bilayer capacitance/pseudocapacitance balancing index. These phytosynthesized materials are fairly competitive with other electrode materials in EES devices due to the improvements in the environmentally friendly production of MO and their electrochemical performance.

1. Introduction

In 1998, Anastas *et al.*[1] proposed 12 principles based on the aspect of "Green Chemistry" to satisfy the requirement of safety, economy, and environmental friendliness, which is devoted to meeting the objective of good yield and benefit as well as lowering the formation of waste and hazardous substances. In this case, green chemistry is one of the impressive areas of research to minimize the adverse effects on society and the environment during the reaction process through chemical methods, including reactants, reaction environment, reaction products, and additives used as catalysis in the reaction products. Biogenic synthesized materials possess improved properties with good chemical reactivity, showing wide scope for the synthesis and refinement of materials in the nano-scale regime. Furthermore, biogenic synthesis is economical, simple, and non-hazardous. In this case, many metal and metal oxide nanoparticles (Ti, V, Cr, Mn, Fe, Co, Ni, Cu, Zn, Pt, Au, and Ag) have been synthesized using green methods.[2] Green-synthesized nanoparticles (NPs) play a vital role in various applications such as catalysis, drugs, medications, sensing,

[a]*Department of Chemistry, School of Advanced Sciences, Vellore Institute of Technology, Vellore-632 014, India. E-mail: ksanthakumar@vit.ac.in*

[b]*Inorganic and Physical Chemistry Laboratory, CSIR-Central Leather Research Institute Chennai, 600 020, India*

environment remediation, electronics, mechanical industry, and energy harvesting.[3] The plant-mediated synthesis of NPs features several advantages, including being quick, inexpensive, and easy to operate with plentiful resources. As a result, it has attracted considerable attention from researchers globally. Plant extracts also have strong biocompatibility, biodegradability, environmental friendliness, and low cost. In addition, they also endow NPs with a stable protective barrier, which prevents their aggregation.[2] However, phytosynthesis is associated with issues including the extraction of the crude materials, long reaction period, quality of material and low yield. For instance, the raw materials are not widely available, the reaction time is long, and the particle geometry and size of the product are highly homogeneous, and due to these parameters, the industrial production and large-scale application of green-synthesized nanoscale metals pose a challenge.[3]

People are becoming more aware of sustainable energy because green energy and energy conservation have increased gradually worldwide due to the revolution of modern science.[4] Consequently, the demand for viable and sustainable energy sources has skyrocketed.[5–7] Sustainability is one of the best paths to meet the needs of the future and achieve well-balanced economic growth, environmental protection, and social well-being without any fluctuations. To reduce the scarcity of fossil fuels and their detrimental effects on the environment, it is critical to develop ecological and sustainable energy storage techniques. Due to their safety and environmental friendliness, greener-based energy storage devices have attracted significant attention and are preferred as the next generation of "green energy storage systems".[8] This has prompted researchers to develop greener sustainable electrochemical energy storage technologies such as batteries and supercapacitors. According to the comparison between supercapacitors and batteries, both play important roles as energy storage systems, for instance, a commercial battery can deliver ~180 W h kg^{-1} energy density, whereas a supercapacitor delivers only ~10 W h kg^{-1} energy density. Alternatively, a capacitor can attain a higher power and larger cyclic stability by millions of times based on its surface storage mechanisms compared to a battery, which can attain only a thousand by intercalation mechanism.[9,10] Hence, batteries are excellent for long-term charge and discharge. Inversely, a supercapacitor is excellent for the storage of a larger amount of energy and rapid discharge.

Battery electrodes are purely based on ion intercalate mechanisms followed by a faradaic charge transport process to generate energy capacity (mA h kg^{-1}), and hence their capacity is limited by solid-state ion diffusion and stores the charge in the form of a chemical reaction. Conversely, supercapacitors depend on the formation of an electrical double layer at the electrode/electrolyte interface by the electrostatic force of interaction or surface/surface near faradaic charge transport method between the electrolyte ions and electrode materials (pseudocapacitor) and store the charge in the form of an electric field. Unlike batteries, the charge storage can occur very fast in supercapacitors. However, despite their faster charge storage, the energy density of supercapacitors remains poor.[11–13]

The history, uses, constructional concepts, and principles of supercapacitors have been previously reviewed by various researchers. Alternatively, phytosynthesized-based materials for supercapacitor applications with the mechanism of phytosynthesis have not yet been the subject of a thorough review article (Scheme 1). A thorough evaluation of this subject is required and timely, as evidenced by the expanding number of related research studies. As a result, this primary topic of this review is on phytosynthesized materials, with a focus on their production and functionality. The main focus of this review is a detailed

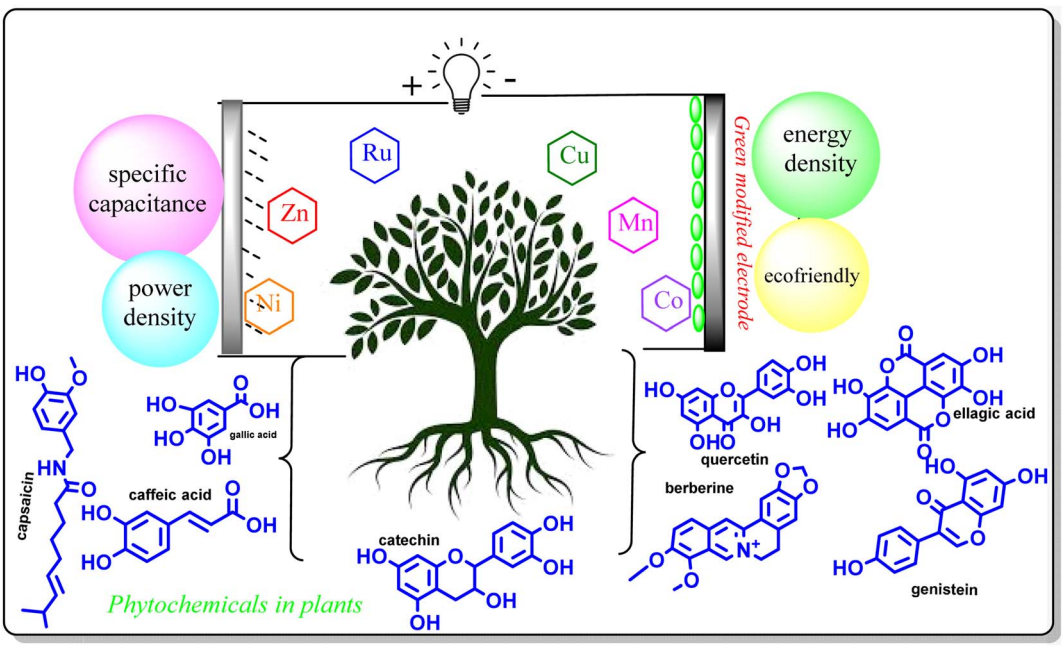

Scheme 1 Phytosynthesis of nanoparticles and their subsequent use in supercapacitor applications.

survey of greener materials. We attempt to summarize most of the papers published in this field. In short, in this review, we present an outline of green-synthesized, especially plant extract-mediated metal and metal oxide nanoparticles for the fabrication of high-performance supercapacitor electrodes because plant-mediated synthesis is a simpler method compared to the handling of microorganisms or fungi-mediated synthesis. Initially, we explore the importance, advantages, and factors influencing the mechanism of green synthesis. In addition, we briefly discuss supercapacitors and their mechanistic aspects, and finally present an outlook of green-synthesized nanoparticles for supercapacitor applications. A summary of supercapacitors may aid in the comprehension of their arrangement, operation, development, benefits and drawbacks, the market landscape, and emerging technologies. SCs are energy storage devices with a variety of noteworthy characteristics, such as elevated power density and specific capacity, extended cycle life, quick charge and discharge speeds, cost effectiveness, environmental friendliness and high safety. Because of the growing interest in portable and flexible electronics, as well as the increasing need for energy-efficient products, SCs are being extensively investigated. Compared to fuel cells and electrochemical batteries, they offer several advantages, including faster charging periods. Supercapacitors (SCs) are significant because of their unique characteristics, which include long cycle life, high strength, and environmental friendliness. They are also important because they exhibit basic equations with traditional capacitors, and they can achieve high capacitance by using electrode materials with high specific surface area and thinner dielectrics.[12]

2. Impacts of phytosynthesis (PS)

Since it was realized that nature can function as a nano-factory, interest in the plant world has been rekindled, as shown in Fig. 1a. The enormous plant diversity is responsible for the lack of investigation in this field, indicating that plants with the potential for synthesizing NPs have largely gone undiscovered. The green synthesis (GS) idea is still in development, which has a satisfactory synthesis rate and has demonstrated great diversification in the taxonomic groups of explored plants. This strategy makes it possible for humans to use nanoproducts securely. However, although green synthesis is interesting and challenging, it requires a brief understanding of the phytonutrient evolutionary properties of plants, which are related to the effectiveness of green synthesis. The phytonutrients of angiosperms, gymnosperms, and pteridophytes all share bioactive components belonging to phenolic, alkaloid, flavonoids, and terpenoid groups, which can play a significant role in the reduction process.[14–17]

A compelling field in nanoscience and technology over the past few decades has been novel synthesis approaches/methods for nanomaterials such as metal and metal oxide nanoparticles, quantum dots (QDs), carbon nanotubes (CNTs), graphene, and their composites. Two distinct basic principles of synthesis (*i.e.*, top-down and bottom-up methods) have been studied in the literature to produce nanomaterials with the desired sizes, shapes, and functionalities.[5] In the former, nanomaterials and nanoparticles are created using a variety of synthesis methods, including lithography, ball milling, etching, and sputtering. Numerous techniques, such as chemical vapor deposition, sol–

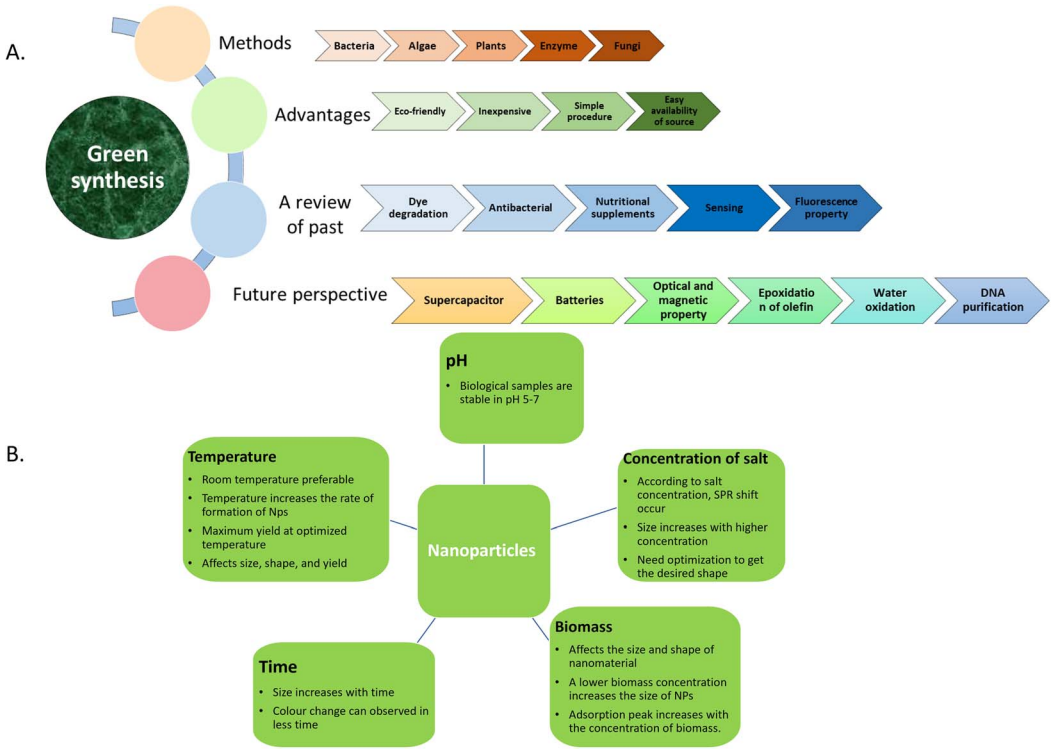

Fig. 1 (a) Importance and applications of green synthesis. (b). Factors affecting the biosynthesis of nanoparticles.

gel processes, spray pyrolysis, laser pyrolysis, and atomic/molecular condensation, are also used in the bottom-up strategy. In this case, the desired parameters of the nanomaterial (size and shape) can be optimized by varying the concentration of chemicals and the reaction parameters such as temperature, pH, solvent, time, and concentration of metal ions. However, the synthesized nanomaterials may exhibit certain limitations or challenges when implemented in actual or specific applications, as follows: (i) poor stability in harsh surroundings; (ii) lack of awareness of their fundamental mechanism and modelling aspects; (iii) exposure to toxic substances/toxicity; (iv) extensive screening requirements; (v) requirement for trained operators; (vi) issue with system assembly and framework; and (vii) recycle/reuse.[18] Thus, to overcome these drawbacks, the new era of PS methodology has been receiving increasing attention in research and development of enhanced high-performance materials by greener method due to its non-toxicity, low cost, and simple procedure. Green synthesis can be accomplished using algae, bacteria, yeast, fungi, and plant extract. In particular, plant extract-mediated green synthesis is considered one of the best methods due to the predictions of the plausible mechanisms of the bioreduction process. The presence of a plethora of natural compounds such as proteins, alkaloids, flavones, and polyphenols can act as natural reducing and capping agents to form NPs from metal ions. Furthermore, the size, shape, and properties of NPs can be optimized using varying biomolecules present in plants such as the active ingredients in their stems, flowers, seeds, bark, leaves, fruits, and peel.[19]

3. Phytonutrients in plant extracts

Extracts that are used to biosynthesize metallic nanoparticles contain several different types of secondary metabolites, namely carbohydrates, amino acids, organic acids, vitamins, and proteins, which are among the bioactive compounds that compose the majority of the secondary metabolites found in plant extracts and are involved in the formation of metallic NPs. These molecules aid in reducing metal ions and stabilizing the NPs.

A class of polyphenolic chemicals known as flavonoids has the power to efficiently chelate metal ions, transforming them into nanoparticles (NPs). Their capacity to form NPs is attributed to their abundance of functional groups, such as numerous hydroxyl and carbonyl groups. The high phenol and flavonoid content in aqueous plant extract makes it simple for M^{+} to undergo bioreduction to M^{0}.[20] It has been suggested that the release of reactive hydrogen atoms, which results in metal ion reduction, occurs as a result of the keto–enol tautomeric transition of flavonoid.[20] Catechol, catechin, caffeic acid, rutin, and quercetin have strong chelating properties due to the presence of a carboxyl group and hydroxyl groups connected to the C3 and C5 sites, and C30–C40. Flavonoids chelate the Fe^{2+}, Fe^{3+}, Cu^{2+}, Zn^{2+}, Al^{3+}, Cr^{3+}, Pb^{2+}, and Co^{2+} metal ions, reveling why flavonoids are so easily adsorbed on the surfaces of developing NPs. As a result, they can influence the nucleation stage of NP formation, while also restricting the aggregation of NPs and mediating their bio-reduction.[21] Protein amine groups, hydroxyl and carboxyl groups of polyphenols, flavonoids, amino acids, hydroxyl groups of polysaccharides, and carboxyl groups of organic acids all chelate metal ions and prevent superoxide from catalyzing the formation of metallic NPs (flavonoids and polyphenols can reduce metal ions). Additionally, in green synthesis, flavonoids and polyphenols can function as reducing and electrostatic stabilizing agents.[20]

Alkaloids are one of the most reported classes of natural products, which are naturally occurring nitrogen-containing substances found in a variety of plant parts, such as seeds, roots, flowers, leaves, and fruits.[22] There are already several alkaloid-class medications on the market, including morphine, quinine, and berberine.[23] Terpenoids, which are low molecular weight aromatic and aliphatic substances, play a crucial role in the creation of Ag nanoparticles. Terpenoids are hypothesized to behave as surface active molecules, which aid in stabilizing and reducing the aggregation of nanoparticles, while the exact mechanism by which they contribute to nanoparticle production is uncertain. Plants produce numerous secondary metabolites that are necessary for the formation of metal and metal oxide nanoparticles, such as terpenoid-rich essential oils. According to several studies, the secondary metabolites in plant-derived essential oils serve as the main producers of nanoparticles.[24,25]

4. Factors affecting PS and its mechanism

Various factors such as temperature, time, pH, biomass, solvent, natural composition, and stirring speed can play a key role in the optimization of PS (Fig. 1b). Controlling the form of biosynthesized NPs is a challenging task because of the multitude of components in bio-sources. The ratio between the precursor and capping agent concentration usually regulates the size and creation of nanoparticles. When the percentage is extremely high or extremely low, aggregation is more likely to occur, which may lead to polydisperse or irregularly shaped particles. If the reaction is carried out at a higher temperature, the rate of the formation of nanoparticles increases but the biomolecules cannot withstand higher temperatures, which affects the size and shape of the material. As the reaction duration increases, the size of the prepared material increases. Also, pH plays a crucial role in the biomolecule-mediated synthesis of materials because the bioactive ingredients can remain stable at the optimized pH. The concentration of the salt precursor causes a shift in the SPR (surface peak resonance) peak and the size range increases with a higher concentration of precursor, and particularly in the case of biomass, the adsorption peak of the material increases with an increase in the concentration of the bio-extract, where the higher the concentration of bio-extract, the lower the size range of the material. The optimization factors that affect the biosynthesis of metal and metal oxide nanoparticles include temperature, pH, reaction duration, agitation, metal salts, and plant extract concentration. Our group achieved the desired form and size of NPs with the aid of optimized parameter settings, given that the appropriate monodispersity, stability, and biocompatibility of manufactured NPs depend on their optimization.[26]

4.1 Effect of light source

It has been demonstrated that repeated exposure to sunshine has an impact on the rate of biosynthesis. AgNPs were exposed to sunshine and it was found that this shortened the biosynthesis process from 12 h to just 5 min. The effects of altering the frequency of the light used to illuminate the metallic NPs were also examined. In this case, different colored cellophane paper filters were used to wrap the reaction vessels. It was shown that the growth of smaller spherical AgNPs was encouraged by the violet filter. The *in situ* production of AgNPs with light is one of the advantageous procedures that has recently emerged. It is highly adaptable and selective, and it can also control the morphology of the generated AgNPs.[27]

4.2 Effect of pH

Numerous studies have shown that pH is a key factor in the production of NPs, such as colloidal gold. According to the study by Gardea-Torresdey *et al.*,[28] pH affects the size of NPs. This finding was supported by Mock *et al.*,[29] demonstrating that NPs can develop in a variety of sizes and forms depending on pH. Because extracts from various plants and different portions of the same plant exhibit varying pH values (which are inversely related to size), as suggested by numerous researchers, optimization of the synthetic process is necessary for the efficient generation of NPs. It is well known that pH has an impact on the shapes and sizes of nanoparticles.[30] According to Sathishkumar *et al.*,[31] when the concentration of the extract and pH value increased (pH value was 5 or above), the yield of the prepared silver nanoparticles using *Cinnamomum zeylanicum* bark extract increased. Higher pH values also promoted the synthesis of more spherical nanoparticles. Alternatively, in other cases, acidic conditions encouraged the creation of spherical monodispersed silver nanoparticles. Lower pH levels have also been reported to enhance the formation of bigger nanoparticles. For example, rod-shaped gold nanoparticles produced from the biomass of *Avena sativa* at pH 2 were larger (25–85 nm) than that produced at pH 3 or 4 (5–20 nm).[32]

4.3 Effect of temperature

The yield of silver nanoparticles and the reaction temperature are directly related.[31] Gericke *et al.*[33] found that the yield of gold NPs increased with an increase in temperature. The size and shape of NPs are significantly influenced by temperature. Andreescu *et al.*,[34] noted a quick synthesis rate of AgNPs at high temperatures. Lengke *et al.*[35] believed that effective crystal growth (111 faces) was responsible for this phenomenon. This occurred as a result of Ag atom build-up on the cubic (100) faces rather than the nucleation of new silver crystals at higher temperatures. Sathishkumar *et al.*[31] observed that surface plasmon resonance increases with temperature and concluded that there is a positive correlation between nanoparticle production and temperature. Liu *et al.* investigated how temperature affects the constant k_1 (nucleation kinetics) and k_2 (growth kinetics). Higher temperatures encourage both nucleation and growth because k_1 and k_2 increase with temperature. However, k_2 increases roughly linearly with an increase in temperature, whereas k_1 increases nonlinearly. Therefore, if the precursors are sufficient, the particle size increment follows a similar pattern to the increase in k_2. The k_1 constant only impacts the number of nanoparticles and has little effect on particle size. Although explosive nucleation will consume a significant amount of Ag^+, if the precursor supply is insufficient, the development would be constrained. The size of AgNPs increased significantly from 70 °C to 80 °C, but it decreased dramatically from 80 °C to 90 °C. Besides the size and shape when the temperature increases, the capacitance of the synthesized material also increases.[36,37]

4.4 Effect of contact time

Previous research suggested that the incubation period also affects the generation of NPs. Dwivedi *et al.*[38] proposed that the UV absorption peak intensities increase with an increase in contact duration in their study on *Chenopodium* leaf extract. They reported that NPs started to develop within a quarter of an hour following the reaction, while after 2 h, not many changes were observed. A different investigation noted that the tansy fruit-mediated synthesis of silver and gold NPs started within 1/6th of an hour following the reaction. Additionally, they found that an increase in the contact time explained the sharpness of the peaks in both Ag- and AuNPs.[39] According to Veeraswamy's group,[40] an ideal time frame is required to complete the nucleation process, and subsequently achieve nanoparticle stability because the newly created nanoparticles are unstable. In their experiment, it was discovered that 60 min was the ideal amount of time for the reaction to be finished and produce silver nanoparticles. Similarly, the Ghoreishi group[41] demonstrated the requirement of the optimum reaction time to produce stable silver and gold nanoparticle using *Rosa damascene*.

5. Plausible mechanism of phytosynthesis

Simple hydrocarbons, monoterpenoids, isoprenoids, carotenoids, sesquiterpenoids, turpentines, and sterols are the fundamental constituents of phytochemicals (Fig. 2). These small molecular building blocks can be broken down into more complex metabolites, such as the phytol tail in chlorophyll. These are the important molecules that make it possible to synthesize NPs from stable plants. These substances can cap NPs, which are essential for aggregation, inhibition, and stopping their growth. Due to the differences in their reduction ability, they also affect the size and form of NPs.

At various stages of the reaction, the extract is combined with metal precursor solutions. The factors that determine the properties of the plant leaf extract (such as the types of phytochemicals, their concentrations, the concentration of metal salts, pH, and temperature) can be employed to regulate the production and stability of nanoparticles as well as the rate of their formation.[42] In contrast to fungi and bacteria, which require a longer incubation period, the phytochemicals found

in plant leaf extracts have amazing ability to reduce metal ions in a considerably shorter amount of time.[36] As a result, plant leaf extracts are regarded as a superior and safe source for the creation of metal and metal oxide nanoparticles. Moreover, the plant extract plays a dual role of stabilizing agent and reducing agent. Additionally, the composition of the plant leaf extract is crucial for the creation of nanoparticles; for instance, the quantity of phytochemicals in various plants varies. Flavones, terpenoids, sugars, ketones, aldehydes, carboxylic acids, and amides are the primary phytochemicals found in plants that are involved in the bio-reduction of nanoparticles.[43]

The different functional groups found in flavonoids have an improved capacity to reduce metal ions. In flavonoids, tautomeric transformations occur when their enol-form changes to the keto-form, releasing a reactive hydrogen atom. Metal ions are reduced into metal nanoparticles to carry out this operation. The enol-to-keto-transformation in sweet basil (*Ocimum basilicum*) extracts was crucial for the production of biogenic silver nanoparticles.[44]

Plant extracts contain sugars such as fructose and glucose, which can contribute to the creation of metallic nanoparticles. It should be noted that the fructose-mediated synthesis of gold and silver nanoparticles produced monodisperse particles, but glucose was capable of taking part in the formation of metallic nanoparticles with varying sizes and forms.[45]

Plant extracts have been used to create green nanoparticles, and the FTIR study of these particles showed that they are frequently linked to proteins. Additionally, different amino

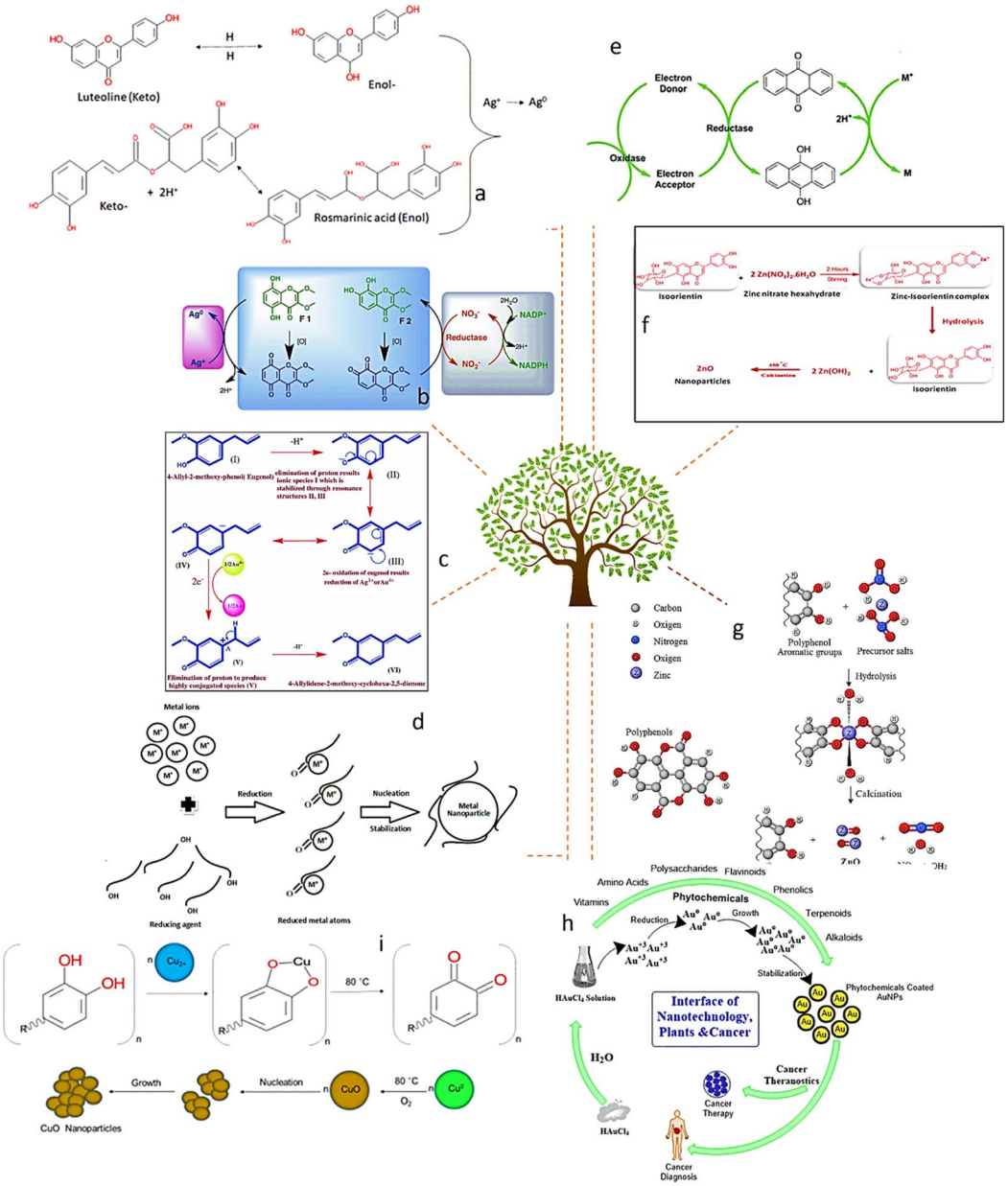

Fig. 2 Proposed plausible mechanism for the phytosynthesis of metal nanoparticles (a and i),[52] (b),[52] (c),[53] (d),[55] (e),[56] (f),[57] (g)[58] and (h).[59]

acids reduce metal ions in different ways. According to L. Clem Gruen,[46] the amino acids cysteine, arginine, lysine, and methionine are particularly effective at binding to silver ions. In 2010, Tan *et al.*[47] evaluated each of the 20 natural amino acids to determine their effectiveness in reducing Au^0 metal ions. Plant extracts contain biomolecules such as proteins and carbohydrates that function as reducing agents to encourage the creation of metallic nanoparticles. Additionally, the proteins found in plant extracts with functionalized amino groups ($-NH_2$) can take part in the reduction of metal ions. Metallic nanoparticles can be produced by the functional groups (such as –C–O–C–, –C–O–, –C═C–, and –C═O–) found in phytochemicals such as flavones, alkaloids, phenols, and anthracenes.[48]

Huang *et al.*[49] reported that the FTIR absorption peaks at 1042 and 1077, 1606 and 1622, and 1700–1800 cm^{-1} indicate the stretching of –C–O–C– or –C–O–, –C═C–, and –C═O, respectively. Kesharwani *et al.*[50] reported that photographic films were overlaid with a silver bromide emulsion. Subsequently, the silver bromide film was sensitized by light, and when it was exposed, it was placed in a hydroquinone solution to further oxidize the silver ions to produce quinone. The silver metal still present in the emulsion replaced the silver ions. Based on the chemistry of photography, our group predicted that the principal reducing agent for the reduction of silver ions to silver nanoparticles through non-cyclic photophosphorylation would be hydroquinone, plastohydroquinone, or quinol (an alcoholic molecule). Therefore, our work demonstrates that plants produce metallic nanoparticles extracellularly using the biomolecules and heterocyclic chemicals found in their extract.

However, the precise underlying mechanism for producing metal oxide nanoparticles using plant extracts is still not well understood. Metallic nanoparticle synthesis from plant extracts typically occurs in three phases, as follows: (1) the activation phase (bioreduction of metal ions/salts and nucleation process of the reduced metal ions), (2) the growth phase (spontaneous combination of small particles with greater ones) *via* a process known as Ostwald ripening, and (3) the final phase, *i.e.*, the termination phase (defining the final shape of the nanoparticles).[51,53,54] It is anticipated that green synthesis will be a promising method for the manufacture of electrode materials for supercapacitors with acceptable energy storage properties due to its inherent benefits over chemical methods.

Consequently, to better comprehend the topics that will be covered, it is crucial to understand supercapacitor technology before moving to the topic of discussion. These details are provided in the following section.

6. Energy storage supercapacitor technology

Energy storage and conversion devices such as batteries, supercapacitors, and fuel cells deal with the potent conversion of electrical and chemical energies. A typical supercapacitor consists of two electrodes with opposing polarities, which are constructed using porous, high surface area electroactive materials and ionically coupled by electrolytes and divided by a porous membrane that is packed with electrolyte. As seen in Fig. 3, the complete setup is kept enclosed in an insulating jacket[60,61] and the basic terminology is presented in Table 1.

The electrodes and electrolyte components employed in various energy devices have a wide range of electrochemical properties, as evident in their reported charging and discharging performances. The typical characterization procedures used to ascertain their electrochemical capabilities are cyclic voltammetry (CV), galvanostatic charging discharging measurements (GCD), and electrochemical impedance spectroscopy (EIS). The electrochemical reversibility of the system is revealed by a distinct CV plot, which also determines the functional electrochemical window from the current–voltage responses at various voltage sweep rates.[62–64]

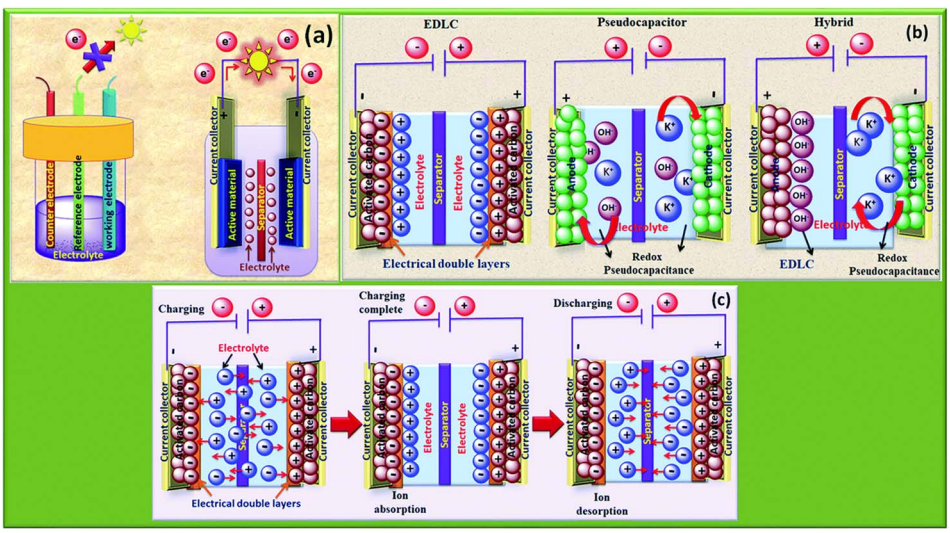

Fig. 3 (a) Conceptual representation of the two- and three-electrode configurations, (b) types of supercapacitors, including hybrid, pseudocapacitor, and EDLC, and (c) charge storage process in EDLCs, including ion absorption and desorption on the surface.[67]

Table 1 Basic terminology

Specific capacitance	Charge storing ability per mass of the system
Specific energy	The energy accumulated per unit mass of the system
Specific power	The energy delivered per unit mass of the system
Capacity	The capacitance response at varying current densities or different potential scan rates
Electrochemical reversibility	Measures the reversibility in the kinetics of charge transfer reactions at the electrode/electrolyte interfaces
Electrochemical window	Voltage limits within the system
Electrochemical stability	Capacitance at a specific voltage, recorded at a constant current to determine the efficacy of the material for long-term cycling

GCD plots help determine the internal resistance, power, and energy densities by displaying the voltage-time variation at a specific current density. The Nyquist plots obtained from EIS studies show a variation in the imaginary *versus* real parts of the complex impedance of individual electrodes or electrochemical cells, offering insightful details about the diffusion of the electrolyte ions at the bulk electrode phase, the charge transfer kinetics at the electrode/electrolyte boundary, and capacitive responses of the system at various AC frequencies. The specific/gravimetric capacitance (C_s) of electrode materials, which is often computed using the eqn (1) and (2) and the data from CV or GCD, is a widely used as an indicator of the ability of a system to store charges.[63]

$$C_s = \left(\frac{1}{sm_{el}}\right)\Delta V \int_{V1}^{Vn} i\mathrm{d}V \quad (1)$$

$$C_s = \frac{1}{m_{el*} \times \left(\frac{\Delta V}{\Delta t}\right)} \quad (2)$$

where $\int(i\mathrm{d}V)$ is the total charge stored, s represents the sweep rate, V_n and V_1 are two voltage limits, m_{el} indicates the electrode mass, I represents the current applied in GCD, and Δ and t represents the discharging time.

Cs is usually used to evaluate the specific energy and specific power using the eqn (3) and (4), respectively:[64,65]

$$\text{Specific energy}(E) = \int Q\mathrm{d}V = \int C\mathrm{d}V = \frac{1}{2}C_{Spt}(\Delta V)^2 \quad (3)$$

$$\text{Specific power } (P) = (E/\Delta t) \quad (4)$$

7. Mechanism of charge storage

The electrochemical mechanisms determine the respective energy storage qualities, where supercapacitors depend on electrochemical processes to store energy. Three different types of charge storage mechanisms have typically been proposed, as follows: (a) non-faradaic double-layer capacitance, which is typically displayed by EDLCs; (b) faradaic, capacitive processes involving electron transfer-mediated charge storage, which are prevalent in pseudocapacitors; and (c) faradaic non-capacitive processes, which are typically observed in battery systems, as indicated in Fig. 3. For a complete understanding of the electrochemical patterns of these EES systems, their CV and GCD fingerprints are highlighted in Fig. 3.[66]

Typically, during charging and discharging operations, EDLCs collect charge through quick ion-adsorption/desorption processes at the interfaces of electrodes and electrolytes and exhibit almost rectangular current–voltage CV and triangular-symmetric GCD graphs, as shown in Fig. 4. Mesoporous carbons, activated porous carbons, carbon nanotubes, graphene, and other porous carbon systems with enormous surface areas fall within the category of EDLC materials. They can successfully withstand numerous charging and draining cycles, while storing charge at ultrafast speeds.[68,69] However, because of their rapid agglomeration, which significantly reduces their practical capacitances, the majority of these materials do not exhibit substantial visible surface areas.

Alternatively, pseudocapacitors encompass almost all varieties of inorganic semiconducting materials, such as metal oxides, chalcogenides, carbides, and nitrides/carboxy-nitrides, as well as well-known organic conducting polymers such as polyanilines, polypyrroles, and polythiophenes and their derivatives.[9,62,68,70] According to extensive research, the capacitive faradaic process in these semiconducting systems arises from continuous electron transfer over a relatively large potential domain as a result of the delocalization of electrons over many dynamic redox states, resulting in energy bands that produce nearly rectangular CV responses as opposed to battery materials, which are made up of isolated redox-active states and provide peak-shaped CV curves.[63,71]

The near-surface faradaic capacitive processes that convey faster charge storage kinetics similar to EDLCs allow pseudocapacitors, despite having a different charge storage mechanism, to exhibit similar CV and GCD profile characteristics to that of EDLCs, as shown in Fig. 4.[13,68]

Compared to EDLCs, pseudocapacitors typically exhibit higher capacitance values. However, they go through significantly less thorough charging and discharging processes, which is why the prefix term "pseudo" is used to distinguish from traditional EDLCs. The third class of supercapacitors, known as hybrid capacitors, typically includes electrode structures that simultaneously exhibit electrostatic and faradaic charge storage processes. In recent years, their use in high-performance supercapacitors has grown significantly.[13,72,73]

It is important to note that the well-defined redox peaks frequently shown in the CV of pseudocapacitors can lead to the unclear identification of their energy storage mechanisms, as shown in Fig. 4. In contrast to batteries, pseudocapacitors exhibit lower variations in peak voltage values and nearly constant behavior with an increase in the voltage scan rate.[9,68]

Utilizing the kinetic data from sweep voltammetry, it is possible to further separate the two. The peak current i' changes with $\nu^{1/2}$ (ν = voltage sweep rate) for diffusion-controlled redox reactions, whereas i' varies directly with capacitive processes. Eqn (5) represents the resulting general expression.[13,73] The

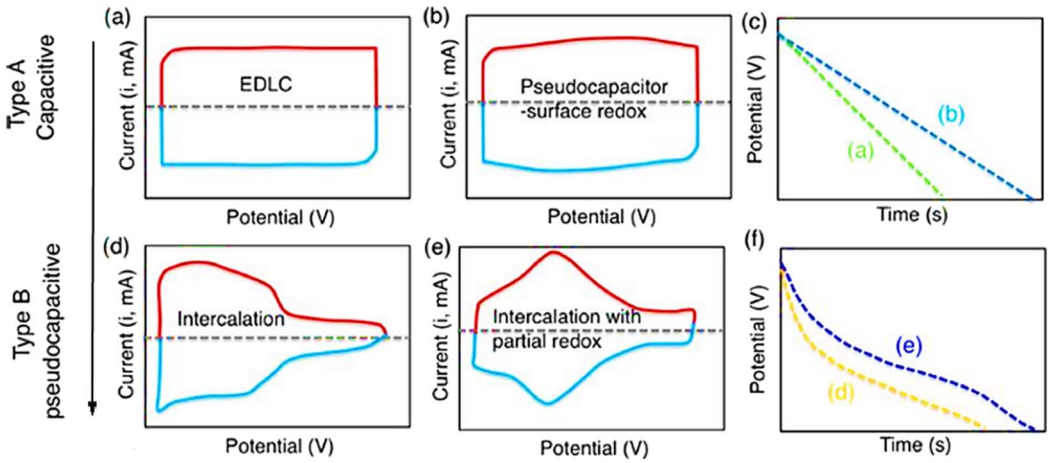

Fig. 4 Systematic representation of CV (a, b, d, and e) and GCD (c and f) for EDLC and pseudocapacitor energy storage systems.[68]

value of x indicates the dominant charge storage mechanism, and the letter "a" denotes a proportionality constant. Pseudocapacitor systems show a value close to unity, whereas values of x 0.5 are frequently recorded for battery materials. Besides the larger coulombic efficacy and faster charge transfer kinetics of pseudocapacitors distinguish them from battery materials.[6,74]

$$i = a \cdot v^x \tag{5}$$

The development of nanoscience and nanotechnology in the energy sector has quickly facilitated the development of innovative conceptualizations to transform and expand the scope of existing energy storage technologies. In addition to enabling outcomes that are extremely close to the theoretical values of electrochemical storage, nanoscale engineering of electrode materials has also promoted quick and effective conversion to electrical energy.[11] As a result, careful examination of the electrochemical processes occurring at the electrode/electrolyte interface of these electrode materials and methodical analysis has revealed new classes of pseudocapacitance, including intercalation pseudocapacitance, redox pseudocapacitance, and underpotential deposition pseudocapacitance, as shown in Fig. 5. In situations in which the electrolyte ions intercalate within the pores or channels of the electro-active materials that undergo faradaic charge transfer with indistinguishable crystallographic phase transformations, intercalation pseudocapacitance is frequently observed, exhibiting faster redox kinetics than battery systems. In the case of intercalation pseudocapacitors, systems such as nano-layered $Ni(OH)_2$, $LiCoO_2$, MoO_3, and V_2O_5 are frequently reported. Alternatively, systems such as MnO_2, RuO_2, and conducting polymers in aqueous electrolytes typically exhibit redox pseudocapacitance, which is related to the faradaic charge transfer processes on the surface of the electrode materials.[75–79]

The third type of pseudocapacitive mechanism, known as "under-potential deposition" (Fig. 5), is when metal ions of one type form an adsorbed single layer on the surface of a different metal well beyond their redox potentials. This type of behavior is seen when a gold or platinum electrode surface forms an

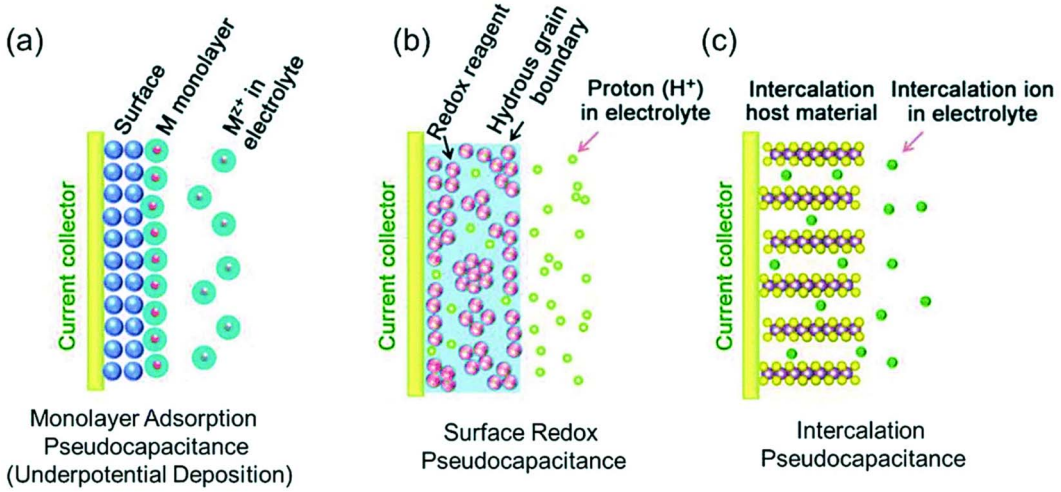

Fig. 5 Demonstration of various types of pseudocapacitive charge storage processes: (a) underpotential deposition, (b) redox pseudocapacitance, and (c) intercalation pseudocapacitance.[82]

adsorbed coating of metal ions such as Cu^{2+}, Pb^{2+}, and Hg^{2+}.[80,81] Depending on the type of electrode and electrolyte materials used in the manufacture of the device, all the aforementioned charge-storing processes frequently operate simultaneously.

Similarly, it has been observed that some redox-active substances, such as $LiCoO_2$, MoO_2, and $NiMoO_4$, typically exhibit battery-type behavior in the bulk phase, but upon dimension reduction and modification, their pseudocapacitive responses become highly distinctive, and are subsequently categorized as "extrinsic pseudocapacitor"; in contrast, "intrinsic pseudocapacitors," such as RuO_2, and MnO_2, are typical pseudocapacitors.[68,70,81]

Furthermore, it should be noted that pseudocapacitive materials fall somewhere between EDLCs and batteries in terms of their ability to store charge and deliver power; as a result, altering their electrochemical properties based on their composition and morphology, specifically, size, shape, crystalline forms, dimensions, and surface character, can accommodate superior qualities, which may eventually result in interesting energy and power outputs in modified energy storage devices.[81,83–85]

Scientists are working to balance these variables to achieve a measurable value of specific energy that is at least as high as that of the widely used rechargeable batteries. The critical electrode material characteristics, as shown in Fig. 4, include the best possible composition, morphology, material dimensions, doping, and chemical functionalization. These characteristics significantly improve the overall energy performance of various EES systems, especially in terms of improved biocompatibility, charge transport characteristics, increased surface area, and mechanical flexibility to withstand extreme environmental conditions.

In addition, using battery and pseudocapacitive materials together when creating supercapacitor cells results in hybrid topologies, which are referred to as "hybrid capacitors," "supercapacitors," and "super-batteries".[9,68,72,86]

They are thought to combine the best qualities of batteries and supercapacitors in a single device. Therefore, developing "smart and diligent electrode materials" that can successfully guarantee all the aforementioned properties for improved supercapacitors is unquestionably a serious task.[87]

8. Criteria for SC electrodes

To improve the performance of electrode materials, several factors should be considered, as follows:

(1) high energy is produced by the high specific capacitance (Sc) at a high mass loading;

(2) broad potential window and chemical stability of the employed electrolytes;

(3) high permeability for quick electron and ion transport, as well as a large surface area for ion adsorption and redox reactions to ensure high power;

(4) high-rate capability is ensured by the high reversibility of the surface/near-surface redox processes;

(5) to achieve high cycling retention, a stable electrode structure and a strong electrode/electrolyte contact are necessary;

(6) ease of preparation, affordability, and eco-friendliness; and

(7) when the electrode materials are assembled into devices, there is a high energy density and power density.

Hybrid supercapacitors are advanced energy storage devices with an asymmetric structure, where the cathode electrode and anode electrode thicknesses are not equal. The cathode electrode plays a vital role in the performance of hybrid supercapacitors. When the thickness of the cathode electrode is increased, the charge–discharge time also increases. This is because a greater thickness of the cathode electrode results in a larger area of the electric double layer in the hybrid supercapacitor. Consequently, this leads to a significant increase in the effective capacity of the hybrid supercapacitor. By understanding the relationship between the thickness of the cathode electrode and its impact on the charge–discharge time, we can optimize the design of hybrid supercapacitors for better performance and efficiency. The charging and discharging time affect the average state of charge (SOC) of the anode electrode. The minimum SOC value indicates the end of the charging process and decreases as the thickness of the anode electrode increases. The anode electrode detaches more ions, leading to an increase in the capacity of the hybrid supercapacitor. The thickness ratio of the anode to cathode electrodes, which is called the thickness ratio, affects the temperature distribution of hybrid supercapacitors. However, this effect depends on the charge–discharge current value. A larger charge–discharge current leads to a more apparent effect. The heat-dissipation capacity of the cathode electrode diminishes as the thickness of the cathode electrode increases, particularly under high current conditions. Hence, selecting the optimal thickness ratio is crucial for optimizing the performance of hybrid supercapacitors. Under the conditions of high loading and elevated temperatures, increasing the thickness of the anode electrode enhances both the power density and heat-dissipation capacity. In contrast, to achieve a greater energy density, it is advisable to suitably increase the thickness of the cathode electrode.[77]

However, few combinations can satisfy all these requirements simultaneously.

9. The impulse for metal oxides as super capacitive electrodes

In the crucial family of pseudocapacitive electrode materials for supercapacitors known as metal oxides (MOs), oxygen atoms are linked to metals. Because of their incompleted subshell and variable oxidation states, MOs exhibit a remarkable convergence of structural, electrical, electrochemical, and mechanical properties. The type of metal and the synthesis of oxide compounds affect the electronic characteristics of MOs. Outstanding qualities that are not possible with their bulk equivalents can be obtained by scaling down MOs to the nanoscale. A high surface-to-volume ratio and increased surface area due to nanoscale shape enable the efficient use of MOs as

electrode materials in energy storage devices. They are desirable materials for supercapacitors due to their high specific capacitance, increased energy density, reversible and quick charge–discharge process, low cost, and environmental friendliness. However, the main issues that need to be solved are their poor electrical conductivity, poor cycle capabilities, low surface area, and low power density. Briefly, transition metal oxides should have the following fundamental properties before they can be used as supercapacitor electrodes: (1) high electronic conductivity; (2) two or more oxidation states that can coexist over a wide potential window without phase change; and (3) quick intercalation/deintercalation of protons or other cations within their 3D-lattice during redox reactions.

10. Materials for SCs

Designing innovative electrode materials for asymmetric supercapacitors is the key to enhancing the performance of supercapacitors. In general, high surface area active materials that store charge in both electrostatic and pseudocapacitive modes are categorized as electrode materials for supercapacitors. High specific surface area, high electronic conductivity, porosity, and electrochemical stability are essential properties of electrode materials that store charge electrostatically through the development of double layers.[9] All the aforementioned conditions are satisfied by carbon-based materials including graphene,[70] carbon nanotubes,[88] carbon onions,[89,90] and activated carbon.[91] The widely varying pore diameters of these materials can be divided into three groups, as follows: macropores (pore size > 50 nm), mesopores (pore size > 2 nm), and micropores (pore size 2 nm).[92] Furthermore, composite materials made of carbon produced from biomass and materials based on transition metals can achieve greater structural and performance benefits than single components, opening up new possibilities for the creation of high-performance SC electrode materials.[93] Perovskites such as $SrFeO_3$, and $SrCoO_3$ have been employed as supercapacitor electrode materials Because of their stable structure, oxygen vacancies, and reversible redox capability, perovskite oxides are considered potential materials for supercapacitors. Their excellent crystallinity, cost-effectiveness, charge storage capacity, electrical and ionic conductivity, and electrochemical activity are also well-known qualities.[36,37,94] It has been concluded that the most effective ion adsorption, and consequently the largest double-layer capacitance occur when the ion size is close to the pore size because pore sizes that are less or larger than the ion size result in a decreased capacitance. The typical range of specific capacitance obtained from EDLCs is 100–250 F g^{-1}, while the energy density of supercapacitor devices based on carbon materials is between 3 and 10 W h kg^{-1}.[95,96] Compared to carbon-based materials, pseudocapacitive materials require extra surface redox processes, which result in 10–100 times greater capacitance, making them more desirable for supercapacitors.[97] An important class of pseudocapacitive materials that have been extensively researched as supercapacitor electrodes are conducting polymers and transition metal complexes. Due to their excellent charge storage capacity, inherent flexibility for flexible electronic devices, large potential window between 1 and +1 V, simple synthesis process, and low cost, conductive polymers, such as polypyrrole and polyaniline, have been extensively researched for supercapacitor applications.[4,64,98] However, during the insertion/extraction process, conducting polymers experience both swelling and shrinkage, which reduce the mechanical stability of the electrodes, and consequently the cycling stability of supercapacitors. In addition to conducting polymers, many transition metal compounds with greater electrochemical stability than polymer-based materials and higher capacitance than carbon-based materials have been studied for supercapacitor applications. Despite the excellent proton conductivity and cycle stability of ruthenium, its restricted availability, toxicity, and high cost have hinder its broad use in industry. Thus, the search for new, less expensive transition metal compounds with improved performances has been accelerated to address this problem. Researchers also concentrate on transition metal elements that are common on Earth and have multivalent states. These transition metal elements combine to generate a variety of oxides, sulphides, selenides, and hydroxides when they are coordinated with other elements such as O, S, and Se as well as functional groups of OH, respectively. Due to their inherent high electrical conductivity, transition metal sulphides and selenides are intriguing materials for supercapacitors, but their practical capacitance and energy density are still low. Transition metal hydroxides also have high theoretical specific capacitance, but their low specific capacitance prevents them from being used widely. Thus, before their extensive commercial exploitation, key factors such as their preparation process, morphology and structure control, cost, and performance must be considered.[96,99]

11. TMO supercapacitors

Previously, transition metals were used for supercapacitor applications to realize good stability with higher energy storage capacity, where they were incorporated as metal oxides, bound with polymers and dopants, and steps were taken to enhance their properties. To date, several applications have been presented for green-synthesized TMOs, which were reviewed before, and thus here we present a summary of green-synthesized TMOs for supercapacitors in Table 2 and Fig. 6(a and b).

11.1 Copper

Copper is a well-known metal due to its unique properties, which include non-toxicity, availability, affordability, and ease of fabrication in the form of nanoscale materials, leading to its use in supercapacitor electrodes. A well-known p-type semiconductor material with a low band gap is cupric oxide or copper(II) oxide. The electronic band gap of CuO is composed of the difference between the valence band energy states and conduction band energy states from the Cu 3d-orbitals. Copper oxide nanostructures are an ideal electrode materials for electrochemical energy storage applications due to their captivating

Table 2 A comprehensive summary of various phytosynthesized MO and MO composites for green supercapacitors[a]

S.no	Electrode material	Sc (F g^{-1})	Capacitance retention (%)	Electrolyte	Power density (W kg^{-1})	Energy density (W kg^{-1})	Ref.
1	ZnO-GO	523.4	86	KOH	—	—	131
2	ZnO	6.318	—	$NaHCO_3$	—	1.062	132
3	ZnO	1.023	—	Na_2SO_4	—	—	133
4	ZnO–Co_3O_4	180	85	KOH	375.3	9.54	134
5	ZnO–CeO_2	431	84	KOH	—	—	110
6	$ZnMn_2O_4$	380	65	KCl	—	—	135
7	ZnO@PdO/Pd	178	—	KOH	3718	3.7	129
8	ZnO-rGO	180	80	KCl	—	—	136
9	ZnO–$CoMoO_4$	294.7	94	KOH	6685.7	8	137
10	rGO/CdCuZnO	882	92	KOH	9482	3.9	138
11	ZnO–Co_3O_4	165	—	KOH	7.5K	4.1	139
12	ZnO	535	92	H_2SO_4	65.624	36.456	133
13	ZnO/PTFE	265	87	KOH	—	—	113
14	ZnO-AC	184	—	Na_2SO_4	—	—	140
15	Zn–C	91	92	Na_2SO_4	1K	32.61	141
16	ZnO-rGO	667	97	KOH	500	43	26
17	CuO	338	—	KOH	—	—	101
18	CuO	2.14	—	$NaHCO_3$		0.171	132
19	CuO-GO	82.1	98	KOH	—	—	102
20	CuONPs/AC	245	99.5	Na_2SO_4	2091.6	45.9	142
21	$CuFeS_2$	501	82	Na_2SO_4	—	—	130
22	Cu_2O	87	74	Na_2SO_4	737	39.3	103
23	CNT@TFcP/Cu	280	80	H_2SO_4			104
24	CuO-rGO	137	—	Na_2SO_4	12K	14	105
25	Cu_2O/RGO	195	79	KOH	4114	37.7	143
26	$NiCo_2O_4$	402	85	KOH	748.8	19.8	116
27	NiO	85.3	—	KOH	—	—	118
28	NiO-PC	780	84	KOH	—	—	117
29	NiO	752	95	KOH	—	—	144
30	TiO_2	804	96	Na_2SO_4	—	—	125
31	RuO_2	209	98	H_2SO_4	—	—	129
32	RuO_2	750	97	KOH	—	—	145
33	Au-NPs	80	93	KOH	—	—	146
34	$LiZnVO_4$	88.7	92	KOH	0.51K	12.3	124

[a] GO-Graphene oxide; r-GO-reduced graphene oxide; NPs-nanoparticles; CNT@TFcP/Cu-carbon nanotube@tetraferrocenylporphyrin/copper nanohybrid; PTFE-polytetrafluoroethylene; PC-porous carbon; AC-activated carbon; and C-carbon.

characteristics such as outstanding stability, endurance, and enviable electrochemical properties.[100] Due to its high surface-to-volume ratio and quantum-size effects, CuO show a wide variation in characteristics compared to other metal oxide systems with a reduction in its dimensions. The investigation of the characteristics and structure of CuO and its hybrid nanocomposites demonstrated their viability as suitable electrodes.[74] Recently, Ikhioya *et al.*[101] synthesized copper oxide NPs from *Moringa oleifera* plant extract for energy storage applications, which showed a specific capacitance of 322 F g^{-1} in 1 M KOH electrolyte. Furthermore, they analyzed the different molar concentrations of CuO NPs for enhanced electrode materials. The specific capacitance of the various copper oxide NPs attained was 176 F g^{-1} for 0.2 mol CuO NP, 181 F g^{-1} for 0.3 mol, 322 F g^{-1} for 0.4 mol, 328 F g^{-1} for 0.5 mol and 212 F g^{-1} for 0.6 mol. Ravichandran[102] attempted to decorate CuO NPs prepared using *Clerodendrum phlomidis* with graphene oxide to enhance the specific conductivity of the material. The specific capacitance of CuO was 45.3 F g; however, the decorated CuO-GO attained twice the capacitance of CuO, *i.e.*, 82.1 F g^{-1} at 2 A g^{-1}, and showed appreciable cyclic stability over 10 000 cycle, maintaining 98% of its capacity. Nwanya *et al.*[103] synthesized Cu_2O without any composite, where instead of doping or formation of composite, they used a simpler method to enhance the property of the material. The Cu_2O NPs were synthesized using maize husk and annealed at 600 °C, where interestingly, pure monoclinic CuO nanoparticles were formed by thermally oxidizing pure reddish cubic Cu_2O nanoparticles. After 2500 GCD cycles, the reddish unannealed Cu_2O demonstrated good stability and produced specific capacitances of 252 F g^{-1} at a scan rate of 5 mV s^{-1} and 300 F g^{-1} at a current density of 0.125 A g^{-1}. Additionally, to achieve reasonably high specific capacitances, particularly for the unannealed Cu_2O electrode, the copper oxide nanoparticle synthesis method is beneficial. The unannealed copper oxide device produced a high energy density of 39.3 W kg^{-1} at a power density of 737.0 W kg^{-1} and a specific capacitance of 87 F g^{-1} at a current density of 0.125 A g^{-1} (Fig. 7). This approach combines three key green chemistry principles, as follows: the use of straightforward, low-temperature, economical, and eco-friendly procedures, greener

Fig. 6 (a) Enacted strategies to improve the performance of electrode materials for high-energy supercapacitors. (b) Characteristics of metal oxides and metal oxide composites in SC.

solvents, and sustainable supplies. Therefore, the obtained copper oxide is particularly promising for applications involving electrochemical storage. In the next step of composite formation, Teimuri-mofrad *et al.*[104] fabricated the pi-position of TFcP, and CNTs interact as a donor and acceptor, functionalizing CNTs (Fig. 8). In the following phase, they created the CNT@TFcP/Cu nanohybrid by synthesizing CuNPs with damson fruit extract and CNT@TFcP. The FT-IR, SEM, and XRD techniques were used to evaluate the crystalline structure, surface morphology, growth of CuNPs on the CNT surface, and structural changes in the as-prepared samples. Additionally, EDX analysis supported the uniform distribution of TFcP and CuNPs on the CNT surface. Through the use of the cyclic voltammetry (CV), electrochemical impedance (EIS), and galvanostatic charge–discharge techniques (GCD), the electrochemical efficacy of the CNT@TFcP/Cu nanohybrid electrodes was investigated. At a current density of 10 A g^{-1}, the CNT@TFcP/Cu nanohybrid showed the specific capacitances of 280 F g^{-1}, with

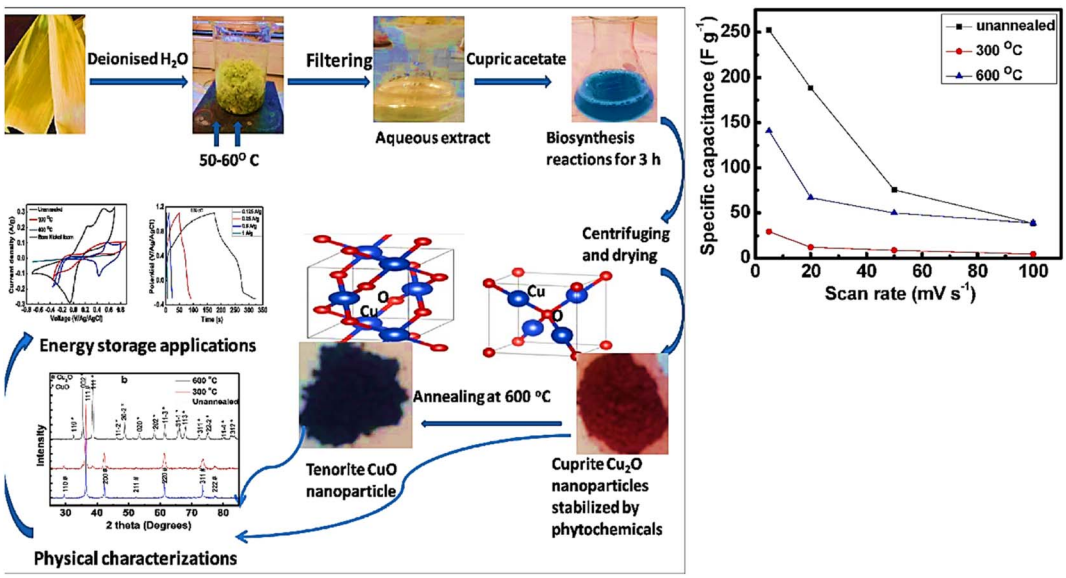

Fig. 7 Schematic of the procedure for the synthesis of Cu_2O NPs and their GCD response at different temperatures.[103]

80% of its initial capacitance was still maintained after 3000 cycles of cyclic voltammetry. The findings demonstrate that the CNT@TFcP/Cu nanohybrid capacitance is enhanced by the presence of nanostructural Cu particles and Fc as an electroactive material. Consequently, a new prospective route for the development of high-performance electrode materials for supercapacitors is provided by the ternary CNT@TFcP/Cu nanohybrid. In 2016, Sudhakar[105] synthesized CuO from *Piper nigrum* and formed a composite with rGO (Fig. 9), showing the specific capacitance of 137 F g^{-1}. Similarly in 2016, Sharath *et al.*[143] also synthesized Cu_2O-rGO from mango bark extract, and the specific capacitance of the synthesized material was 190 F g^{-1}, which is similar to that reported by the Sudhakar group.

11.2 Zinc

Due to its benefits of high hypothetical energy density, exceptional chemical and thermal stability, green and ecological safety, and low cost, Zn has attracted interest from numerous scientific associations. The findings demonstrate that the precise surface area, shape, and micro/nanostructure of Zn have

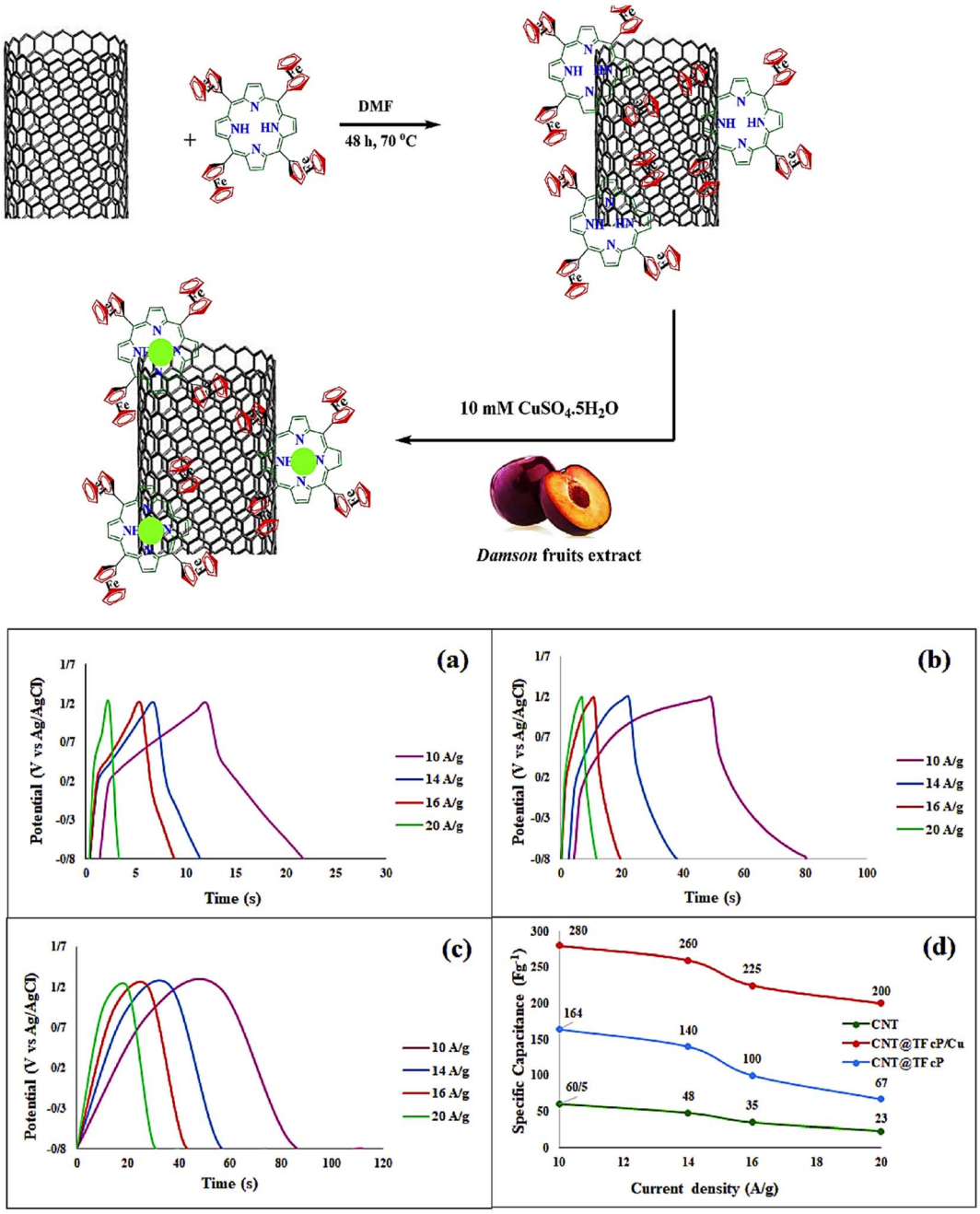

Fig. 8 CNT@TFcP/Cu nanohybrid synthesized using CuNPs prepared using *Damson* fruit extract and its response (a) the GCD curves of the CNTs (b) the GCD curves of the CNT@TFcP nanohybrid (c) the GCD curves of the CNT@TFcP/Cu nanohybrid (d) the specific capacitance values curves *vs.* the current density.[104]

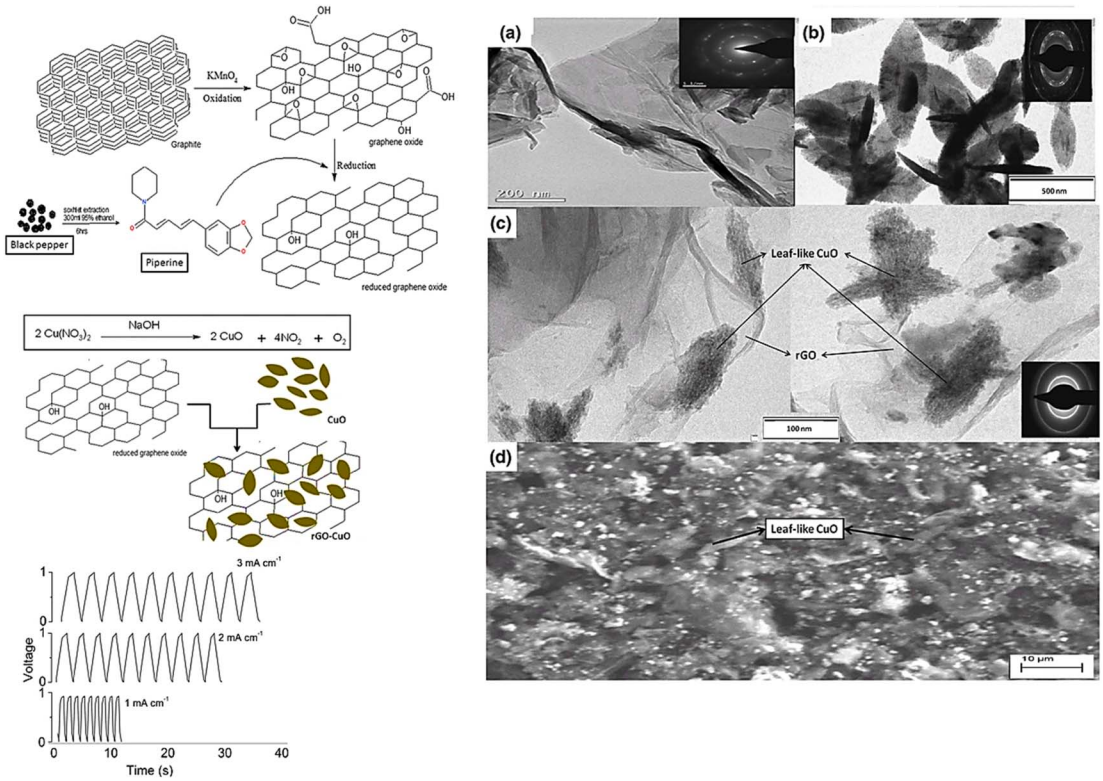

Fig. 9 CuO from *Piper nigrum* with rGO composite leaf-shaped electrode material for energy storage system and the TEM and SAED of rGO (a), CuO (b) and rGO–CuO (c); (d) SEM image of rGO–CuO.[105]

a substantial impact on its electrochemical behavior. When utilized as conductive channels in composite materials, Zn nanostructures can aid in the movement of electrons and the storage capacitance. A detailed analysis required a large amount of time to explore and summarize the most recent advancements in Zn-based materials.[106] The development of a particular class of Zn-based materials was the main focus of the most recent review publications. However, the direct development of Zn-based materials and additional battery-type electrodes for SCs will be difficult without a complete, real-time evaluation of all Zn-based resources in SCs.[107] Herein, we deeply delve into the recent use of zinc-based materials, their energy storage mechanisms, and preparation methods in SC. The present research state of Zn-based materials utilized in SCs is identified using emerging trends and notable achievements.[66] Our team synthesized ZnO NPs from *L. nepetifolia* for electrochemical supercapacitor applications with an average size of 25 nm. The electrochemical analysis of the prepared reduced graphene oxide with zinc oxide (rGO-ZnO) nanocomposite revealed that it has a high specific capacitance of about 667 F g^{-1} in comparison to the pure zinc oxide nanoparticles (200 F g^{-1}) and good cycling stability over 1000 cycles in KOH medium.[108] Additionally, the synthesized ZnO NPs showed good biocompatibility. Saini *et al.*[109] synthesized ZnO using the seed and bark of *Azadirachta indica* for antibacterial, photocatalytic, and supercapacitor applications. The seed-synthesized ZnO showed the highest capacity of 1.5 F g^{-1}, while that of the bark-synthesized ZnO was 1.2 F g^{-1} with the energy density of 0.119 W h kg^{-1} and 0.1010 W h kg^{-1}, respectively, in 0.5 M Na_2SO_4, where even from the same plant, its different parts showed a different specific capacity. Pure ZnO fails to attain a good specific capacity, and thus CeO_2–ZnO was synthesized using *Hibiscus sabdariffa*.[110] To 25 mL of *Hibiscus sabdariffa* L. flower extract, 2.10 g of $Ce(NO_3)_3 \cdot 6H_2O$ and 1.40 g of $Zn(NO_3)_2 \cdot 6H_2O$ were added separately. To create a gel, the solutions were continuously combined and heated at 80 °C for around 3 h. The crystalline CeO_2–ZnO nanocomposite was created by centrifuging the solid precipitate at 4000 rpm for 15 min, drying it in an oven at 100 °C for 6 h, and then calcining it at 500 °C for 1 h to eliminate any remaining organic materials. The environmentally friendly CeO_2–ZnO nanocomposite, which had a maximum specific capacitance of 431 F g^{-1} at a current density of 1 A g^{-1}, exhibited a remarkable electrochemical performance. The specific capacitance retention of the greenly synthesized CeO_2–ZnO nanocomposite significantly increased after 3000 cycles at a current density of 7 A g^{-1} from 69.7% for pure ceria NPs to 89.4% due to hybridization. Similarly, in 2021 (Fig. 10), the ZnO@PdO/Pd material from *E. Cognata* leaves[111] attained a significant specific capacitance of 178 F g^{-1}. Also, a specific energy density of 3.7 W h kg^{-1} in a KOH electrolyte solution calculated from the charge–discharge. In the case of the ZnO@PdO/Pd electrode, a high-power density of 3718 W kg^{-1} was noted. As a result, the exceptional electrochemical properties of the ZnO@PdO/Pd nanocomposite were revealed. Furthermore, ZnO–Co_3O_4 was synthesized from *E. Cognata* in 2020 by the I. Shaheen[112] group. They reported that the phyto-

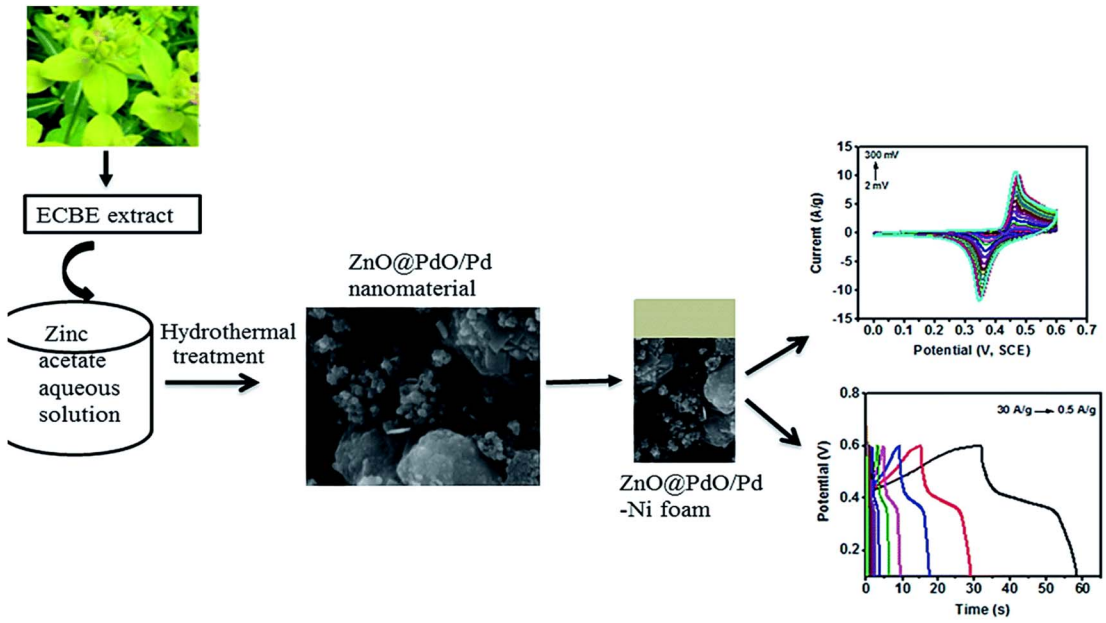

Fig. 10 NF-supported ZnO@PdO/Pd nanomaterial for supercapacitors.[111]

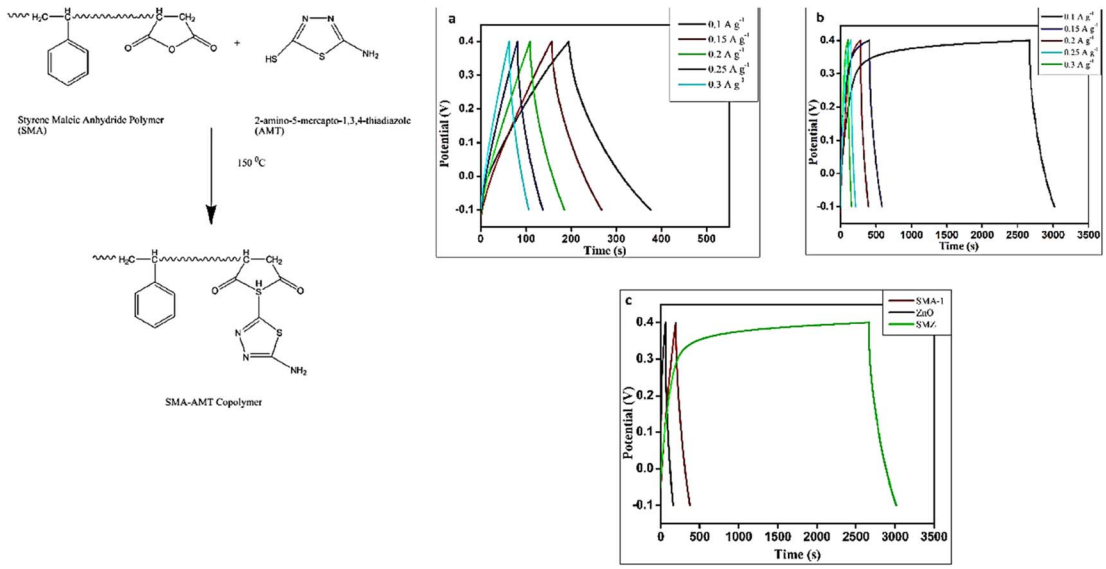

Fig. 11 Thiadiazole moiety used in the polymer matrix of styrene maleic anhydride-mediated ZnO for supercapacitor.[113]

organic functional groups and nanofeatures offered a large number of active sites for charge storage with a specific capacitance of 165 F g^{-1}, as determined by cyclic voltammetry. Using the charge–discharge data, it was determined that the phyto-functionalized nanocomposite possessed an energy density of 4.1 W h kg^{-1} and power density of 7.5 kW kg^{-1}. Besides the formation of Zn composites to enhance the specific capacity, S. Chakraborty *et al.*[113] synthesized a ZnO/polymer nanocomposite for energy storage applications. A thiadiazole moiety was used to effectively modify the polymer matrix of styrene maleic anhydride (Fig. 11). The altered polymer matrix was filled with ZnO nanoparticles that were produced *via* green synthesis. At a current density of 0.1 A g^{-1}, the specific capacitance of the nanocomposite (268.5 F g^{-1}) was greater than that of the bare polymer (145 F g^{-1}) and ZnO nanoparticles (55 F g^{-1}). The nanocomposite exhibited the maximum capacitance retention and great cycle stability.

11.3 Nickel

The electrochemical active components of electrodes are responsible for storing charge, while the current collectors are responsible for transporting it. Some of the most popular modern collectors include aluminum foil, carbon fabric, and nickel foam (NF). Among them, NFs stand out due to their huge active surface area and highly conductive 3-D network. Due to

its high conductivity, Ni is reportedly used as a substrate in supercapacitors and evolution reactions.[114] NF has been widely employed as a supporting substrate for active materials in batteries and supercapacitors due to its huge surface area, high conductivity, high porosity, and remarkable chemical stability in diverse liquid electrolytes.[115] Recently, in 2023, S. Nayak *et al.*[116] synthesized nickel cobaltite using *Moringa oleifera* and proposed the possible mechanism. In this study, green synthesis employing plant extracts was used to create the nickel cobaltite nanomaterial. The structural characteristics of the synthesized nanomaterial were evaluated, and to validate the necessary electrochemical performance parameters of the synthesized nanomaterial, an electrochemical performance analysis was carried out utilizing the GCD, CV, and EIS methodologies. Subsequently, the created nanomaterials and activated carbon were used to construct a hybrid supercapacitor device. The performance of the electrode material was assessed using the same techniques, and the results showed its good energy density, power density, and life cycle stability compared to recent study findings in this field. The results obtained are promising in terms of synthesizing electrode materials sustainably. By including specific substances, such as graphene, carbon nanotubes, and conducting polymers, the electrochemical performances of nanomaterials made by green synthesis can be improved even more. Finally, supercapacitors from artificial nanomaterials[117] and activated carbon demonstrated an improved energy density of 19.8 W h kg^{-1} at a power density of 748.81 W kg^{-1} with a decent retention capacity of almost 85% after 8000 cycles at a current density of 5 A g^{-1}, and the specific capacitance reached 402 F g^{-1}@1 A g^{-1} in 3 M KOH. Conversely, in 2021, another group, synthesized NiO without any composite or doping using guava leaves, and the synthesized NiO NPs were found to exhibit a specific capacitance of 85.31 F g^{-1} in 5 M KOH.[118] Furthermore, S. A. Al Kiey *et al.*[117] attempted to synthesize NiO from banana peel with a porous carbon composite to enhance the properties of raw NiO NPs. The prepared porous carbon NiO composite attained a specific capacitance of 780 F g^{-1} at 5.0 A g^{-1} with a good rate capability of 84.55%. In contrast, the raw NiO NPs exhibited a specific capacitance of only 85.31 F g^{-1}. The superior performance of NiO is due to the presence of porous carbon, which has a 3D porous geometry with high cavities, easily allowing the free movement of ions to attain a good specific capacitance.

11.4 Other MOs for SC

Researchers have focused significant attention on iron oxides as prospective anode materials, particularly Fe_2O_3 and Fe_3O_4 because of their low cost, high specific capacitance, and environmental friendliness. However, their further practical applications are hindered by their poor electric conductivity and high-volume expansion. The aforementioned difficulties can be solved by combining nanostructures with a highly conductive matrix. In this case, high-power density, natural availability, and high theoretical specific capacity are advantages of vanadium-based oxides.[119] However, their utility is restricted by their structural stability and low electric conductivity.[96] The principal vanadium oxides are VO_2, V_2O_3, and V_2O_5, with +5 having the best stability and +4 having the lowest. V_2O_5 has been extensively studied as an electrode material for SC cathodes, but more work needs to be done on VO_2 as an anode material. Its poor conductivity can overcome by anchoring materials based on carbon.[120] T. N. Vinuth Raj *et al.*[121] used *Moringa oleifera* as a reducing agent for the synthesis of an RGO/V_2O_5 nanocomposite, which exhibited a high capacitance of 906 F g^{-1} at a scan rate of 2 mV s^{-1} compared to pure RGO and V_2O_5 due to its surface area and conductivity. Manganese oxide (Mn_3O_4) is another prominent supercapacitor electrode material prepared from olive leaf extract with Na_2SO_4 as the electrolyte, exhibiting a specific capacitance of 583.7 F g^{-1}.[122] RuO_2 is regarded as one of the most promising SC electrodes because of its high theoretical specific capacitance (1700 F g^{-1}), strong electric conductivity (105 S cm^{-1}), and reversible redox reaction. Additionally, RuO_2 has broad applicability in aqueous systems with various aqueous electrolytes because of its strong corrosion resistance to acidic and basic conditions. The two ruthenium oxide phases are crystal phase RuO_2 and amorphous hydrous RuO_2xH_2O. Here, the former has larger active sites and higher capacitance. Among the several metal oxides for SCs, Co_3O_4 cathode materials are considered battery-type electrode materials because they are regulated by diffusion in the electrochemical process in an aqueous electrolyte. Due to its astounding redox reversibility and extremely high theoretical specific capacitance, the Co_3O_4 cathode has undergone intensive development. However, because of its low electric conductivity, its cycling stability and rate capabilities are compromised. Thus, to enhance its electrochemical performances, much effort has been focused on creating nanostructured Co_3O_4 materials. Bimetallic oxides, as opposed to single metal oxides, combine the benefits of multiple metal oxides to function as a supercapacitor. Additionally, it is evident that several pseudocapacitive metal oxide heterostructures have sparked widespread interest among researchers and are currently the subject of study. These heterostructures have been firmly identified as promising structures to improve the electric conductivities and increase the number of active sites in SCs because of the imperfections in their contact surfaces and the synergistic effects of several phases.[10,60,87,120,123] In 2022, Soundarya *et al.*[124] fabricated $LiZnVO_4$ nanoparticles for supercapacitor applications from *Hibiscus rosa sinensis* leaves and reported a specific capacitance of 88.7 F g^{-1} of at a current density of 0.1 mA in 1 M NaOH solution. Another group[125] synthesized flower-like TiO_2 NPs from *Calotropis gigantea* plant leaves and reported a specific capacitance of 804 F g^{-1} at a current density of 1 A g^{-1} in 1 M Na_2SO_4 medium. This is a very good specific capacitance without any composite or doping agent compared with $LiZnVO_4$. This is because each metal plays a role in the SC without dopant or composite and can attain a good specific capacitance, whereas with composites, some metals fail to show capacitance, requiring optimization for better results. N. Kumar Reddy *et al.*[126] synthesized flower-like TiO_2 NPs from *Calotropis gigantea* plant leaves, which acted as catalysts, exhibiting a specific capacitance of 804 F g^{-1} at a current density of 1 A g^{-1} in 1 M Na_2SO_4 medium.

TiO_2-doped RGO nanosheet on carbon cloth obtained from aloe vera and gram seeds exhibited a specific capacitance of 599.9 F g^{-1} with H_2SO_4 as the electrolyte.[127] Xu *et al.*[128] synthesized iron (Fe) decorated with carbon (hydrochar) obtained from bamboo activated by $KHCO_3$ with a high surface area, exhibiting a capacitance of 467 F g^{-1} at 0.5 A g^{-1} when tested in KOH electrolyte and high energy density of 20.31 W h kg^{-1} in Na_2SO_4 electrolyte.

The most promising supercapacitor metal is ruthenium. In 2020, RuO_2 NPs were synthesized by Nisha *et al.* from *Anacyclus pyrethrum* with an average size of 13 nm. The synthesized RuO_2 on carbon paper showed 209 F g^{-1} at a scan rate of 5 mV s^{-1} without any dopants. Another group synthesized RuO_2 from *Aspalathus linearis*, reporting a capacitance of 750 F g^{-1} at 10 A g^{-1} on nickel foam, which confirms that the current collector also plays a major role in the charge storage capacity.[129]

The composite of $CuFeS_2$ was synthesized by[130] Hope *et al.* from mimosa leaf extract, and the appreciable specific capacitance of 501 F g^{-1} at 10 mV s^{-1} in 1.0 M Na_2SO_4 electrolyte was reported. Gold nanoparticles were synthesized from *Solanum nigrum* leaf extract but failed to show an acceptable specific capacitance, attaining only 80 F g^{-1} at 1 A g^{-1} with 93% cyclic stability over 5000 cycles.

12. Limitations

Plant-mediated synthesis provides a variety of advantages, but it also has certain disadvantages. The stability and aggregation, crystal growth regulation, form, size, and size distribution of NPs are the primary issues in plant-mediated synthesis.

Researchers dispute whether plant extract-driven synthesis can match the level of application skill achieved by chemical and physical synthesis. This process requires heating, which increases the cost of producing NPs. Another significant problem with the manufacturing of green NPs is their low yields. Accumulation and resistance are crucial in the biochemical processes and pathways involved in plant heavy metal detoxification to increase NP synthesis at the same rate as chemical and physical approaches. Additionally, there haven't been any cases of NP manufacturing on an industrial scale using plant extracts.[3,38] AgNPs are quickly being recognized as having several advantages across various industries; however, their full toxicological data are still lacking. The exposure, threat posed to human health, and environmental issues caused by AgNPs have not been appropriately addressed. Fabric products release Ag into a sweat, which is influenced by a number of factors, including the fabric quality, amount of silver coating, sweat simulation, and pH. One study found that although keratinocytes are less sensitive than fibroblasts, AgNPs released from commercial dressings largely targeted both cell types. Silver nanoparticles can damage DNA and disrupt cells, leading to the death of fibroblasts and liver cells. According to the likely mechanism of cytotoxicity induction in fibroblasts, AgNPs are involved in the generation of reactive oxygen species (ROS), the translocation of protein to the mitochondria, and the release of cytochrome C into the cytosol.

Different nanoparticles are easily inhaled into the lungs, where they go to the nasopharynx, and eventually the brain. By triggering membrane leakage, decreased mitochondrial activity, and death in germ cells, AgNPs also harm them. Mesenchymal stem cells are susceptible to cytotoxicity from AgNPs even at noncytotoxic concentrations.

13. Applicability of green nanoparticle synthesis

Economic analysis is one of the key factors that must be considered before any new technique is adopted. To discover the best preparation technique, the green synthesis of nanoparticles has also been considered economically. The cost of the materials needed to produce nanoparticles using chemical methods is on the higher side because the starting product is constrained and must be synthesized, while the processes for using green synthesized nanoparticles are less cost-effective. In some circumstances, getting biological resources is simpler and more affordable. Bacterial and fungal nanoparticle manufacturing is feasible due to their ease of management and genetic manipulation. *Verticillium* genus fungal strains and *K. pneumoniae* bacterial strains can be used to produce silver nanoparticles. The use of medicinal plants is justified by the presence of chemical compounds of therapeutic value, namely secondary metabolites with distinct physiological actions in the human body. Surprisingly, AgNPs produced by biological means exhibit great yield, solubility, and stability. Finally, green chemical strategies for synthesizing nanoparticles are quite promising.

14. Future scope

Herein, we discussed the state of the art in green synthetic material supercapacitor technologies. The use of existing technology is limited. However, cathodic/anodic electrochromic materials and electrolyte modification for improved charge/discharge reaction have led to the development of green supercapacitors. This technology can successfully overcome the limitations of conventional chemical supercapacitors, particularly for green energy sources. It is typically employed in the creation of next-generation energy storage systems, which need to perform several other tasks in addition to energy storage. The primary materials employed in the early stages of development were transition metal oxides. However, due to their limited electrical conductivity, they exhibit a low energy density and power density. In this case, conductive polymers can be doped with heteroatoms and biomass carbons, which contain a variety of oxidation/reduction sites, to overcome these drawbacks. Specifically, PEDOT, polyaniline, and polypyrrole can be used as active materials in high electrical conductivity type materials because of their exceptional electrical conductivity and ability to work with cathodic materials. Lately, hybrid-type composite active materials blended with conductive polymers and transition metal oxides have been used to optimize their electrochemical performances. However, although green supercapacitors are considered viable substitutes as the next

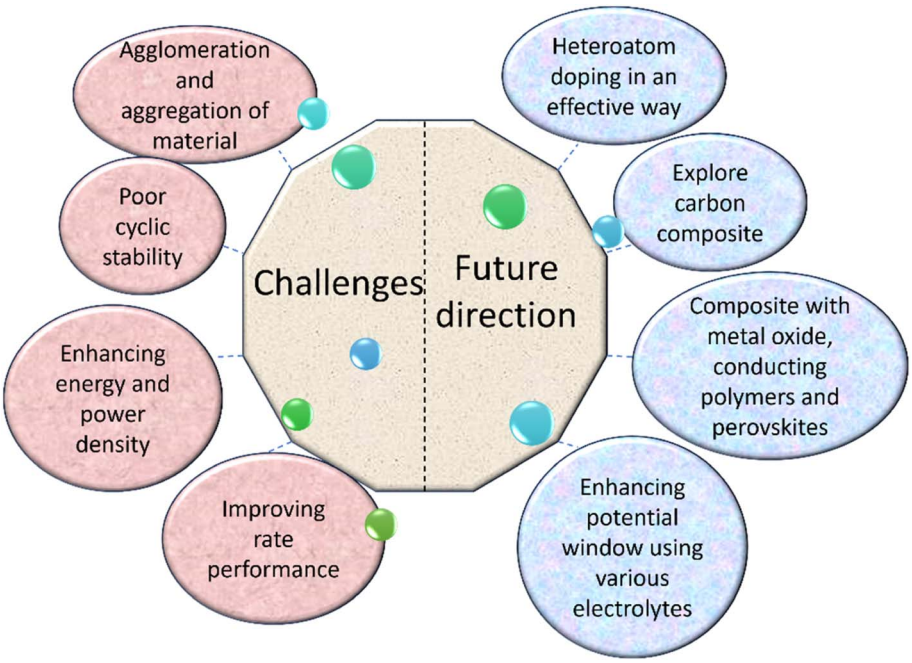

Fig. 12 Challenges and future directions of supercapacitors.

green energy storage systems, their application needs to be further broadened. Firstly, moving away from the method of storing external electric power, it is required to combine large-scale synthesis and storing electric power generated from renewable energy. Given that the green electrode system can be freely adjusted, it is easy to converge with new and renewable energy technology using plant extracts.

Table 3 List of abbreviations used in this review and their terms

	Abbreviation	Term
1	PS	Phytosynthesis
2	GS	Green synthesis
3	NPs	Nanoparticles
4	ZnO	Zinc oxide
5	GO	Graphene oxide
6	r-GO	Reduced graphene oxide
7	CNT	Carbon nanotubes
8	C	Carbon
9	PC	Porous carbon
10	AC	Activated carbon
11	TFcP	Tetraferrocenylporphyrin
12	PTFE	Polytetrafluoroethylene
13	Sc	Specific capacitance
14	MO	Metal oxide
15	SC	Supercapacitor
16	CV	Cyclic voltammetry
17	GCD	Galvanostatic charge–discharge
18	EIS	Electrochemical impedance spectroscopy
19	GCE	Glassy carbon electrode
20	EDLC	Electrical double-layer capacitor
21	EES	Electrochemical energy storage

15. Conclusion

During the preceding years, the phytosynthesis of NPs has witnessed significant developments, and thus this review presented the most recent developments and energy storage applications. In the traditional synthetic technique for fabricating NPs, a large amount of energy is required, and hazardous materials are used, which increase the likelihood that poisonous byproducts may be produced. As a result of the adoption of greener synthesis techniques, this danger can be reduced given that the metal salts are reduced through the use of non-hazardous chemicals. Plant biomolecules reduce metal ions into NPs in a single step. To make this strategy economically feasible and superior to the traditional approaches, researchers need to identify the necessary synthesis routes. The details of the variety of plants that can be utilized to develop an environmentally friendly way to make metallic nanoparticles were discussed. The benefits of using a greener approach over the conventional one were also highlighted to get a green future with green energy technology. It is projected that phytosynthesized NPs will be some of the most promising materials in the future based on their preparation cost, electrical conductivity, cyclic stability performance, and bilayer capacitance/pseudocapacitance balancing index. These phytosynthesized materials are fairly competitive with other electrode materials in EES devices due to the improvements in the environmentally friendly production of MOs and their electrochemical performance. Nonaqueous systems may give way to aqueous systems in the future, which will reduce battery costs and benefit the environment. However, despite their remarkable success and ongoing efforts, MOs will continue to encounter enormous obstacles and possibilities in these domains. Their exceptional qualities can also be used in a variety of other ecologically

relevant fields, including water purification and chemical detection (Fig. 12 and Table 3).

Conflicts of interest

The authors declare no competing financial interest.

References

1 T. Paul and W. J. C. Anastas, *Green Chemistry: Theory and Practice*, oxford university press, New york, 1998.
2 H. Chopra, S. Bibi, I. Singh, M. M. Hasan, M. S. Khan, Q. Yousafi, A. A. Baig, M. M. Rahman, F. Islam, T. Bin Emran and S. Cavalu, *Front. bioeng. biotechnol.*, 2022, **10**, 874742.
3 P. Raveendran, J. Fu and S. L. Wallen, *J. Am. Chem. Soc.*, 2003, **125**, 13940–13941.
4 Z. Yang, J. Zhang, M. C. W. Kintner-Meyer, X. Lu, D. Choi, J. P. Lemmon and J. Liu, *Chem. Rev.*, 2011, **111**, 3577–3613.
5 D. G. Nocera, *Chem. Soc. Rev.*, 2009, **38**, 13–15.
6 S. Chu and A. Majumdar, *Nature*, 2012, **488**, 294–303.
7 T. Nguyen and M. d. F. Montemor, *Advanced Science*, 2019, **6**, 1801797.
8 R. K. Guduru and J. C. Icaza, *Nanomaterials*, 2016, **6**, 41.
9 P. simon and Y. gogotsi, *Nat. Mater.*, 2017, **7**, 845–855.
10 B. E. Conway, *Electrochemical Supercapacitors*, Springer, New York, NY, 1999.
11 V. Augustyn, P. Simon and B. Dunn, *Energy Environ. Sci.*, 2014, **7**, 1597–1614.
12 Z. Yu, L. Tetard, L. Zhai and J. Thomas, *Energy Environ. Sci.*, 2015, **8**, 702–730.
13 D. P. Dubal, O. Ayyad, V. Ruiz and P. Gómez-Romero, *Chem. Soc. Rev.*, 2015, **44**, 1777–1790.
14 R. Ho, T. Teai, J. P. Bianchini, R. Lafont and P. Raharivelomanana, in *Working with Ferns: Issues and Applications*, Springer, New York, 2010, pp. 321–346.
15 Gurav. Kd, B. A. Kore and V. T. Aparadh, *Int. J. Pharma Sci.*, 2013, **2**, 841–843.
16 M. Wink, *Phytochemistry*, 2003, **64**, 3–19.
17 Y. Asakawa, A. Ludwiczuk and F. Nagashima, *Phytochemistry*, 2013, **91**, 52–80.
18 P. Raveendran, J. Fu and S. L. Wallen, *J. Am. Chem. Soc.*, 2003, **125**, 13940–13941.
19 S. Ying, Z. Guan, P. C. Ofoegbu, P. Clubb, C. Rico, F. He and J. Hong, *Environ. Technol. Innovation*, 2022, **26**, 102336.
20 G. Marslin, K. Siram, Q. Maqbool, R. K. Selvakesavan, D. Kruszka, P. Kachlicki and G. Franklin, *Materials*, 2018, **11**, 940.
21 J. Kasthuri, S. Veerapandian and N. Rajendiran, *Colloids Surf., B*, 2009, **68**, 55–60.
22 Y. S. Zhao, X. K. Qian, X. Q. Guan, P. F. Song, Y. Q. Song, R. J. He, M. R. Sun, X. Y. Wang, L. W. Zou and G. B. Ge, *Bioorg. Chem.*, 2020, **105**, 104367.
23 E. Aboutaleb, F. Atyabi, M. R. Khoshayand, A. R. Vatanara, S. N. Ostad, F. Kobarfard and R. Dinarvand, *J. Biomed. Mater. Res.*, 2014, **102**, 2125–2136.
24 S. S. Shankar, A. Ahmad, R. Pasricha and M. Sastry, *J. Mater. Chem.*, 2003, **13**, 1822–1826.
25 S. Hussain, O. Bashir, Z. Khan and S. A. Al-Thabaiti, *J. Mol. Liq.*, 2014, **199**, 489–494.
26 M. Jayaprakash and S. Kannappan, *Arabian J. Chem.*, 2022, **15**, 104324.
27 R. W. Raut, V. D. Mendhulkar and S. B. Kashid, *J. Photochem. Photobiol., B*, 2014, **132**, 45–55.
28 J. L. Gardea-Torresdey, K. J. Tiemann, G. Gamez, K. Dokken, S. Tehuacanero and M. José-Yacamán, *J. Nanopart. Res.*, 1999, **1**, 397–404.
29 J. J. Mock, M. Barbic, D. R. Smith, D. A. Schultz and S. Schultz, *J. Chem. Phys.*, 2002, **116**, 6755–6759.
30 S. P. Dubey, M. Lahtinen and M. Sillanpää, *Process Biochem.*, 2010, **45**, 1065–1071.
31 M. Sathishkumar, K. Sneha and Y. S. Yun, *Bioresour. Technol.*, 2010, **101**, 7958–7965.
32 S. He, Y. Zhang, Z. Guo and N. Gu, *Biotechnol. Prog.*, 2008, **24**, 476–480.
33 M. Gericke and A. Pinches, *Hydrometallurgy*, 2006, **83**, 132–140.
34 D. Andreescu, C. Eastman, K. Balantrapu and D. V. Goia, *J. Mater. Res.*, 2007, **22**, 2488–2496.
35 M. F. Lengke, M. E. Fleet and G. Southam, *Langmuir*, 2007, **23**, 2694–2699.
36 G. Liu, L. Liu, G. Li, S. Wu, J. He, Y. Zhou, M. Demir and P. Ma, *Chem.–Eur. J.*, 2024, **30**, DOI: **10.1002/chem.202303267**.
37 L. Liu, G. Liu, S. Wu, J. He, Y. Zhou, M. Demir, R. Huang, Z. Ruan, G. Jiang and P. Ma, *Ceram. Int.*, 2024, **50**, 1970–1980.
38 A. D. Dwivedi and K. Gopal, *Colloids Surf., A*, 2010, **369**, 27–33.
39 A. Mohammed Fayaz, K. Balaji, P. T. Kalaichelvan and R. Venkatesan, *Colloids Surf., B*, 2009, **74**, 123–126.
40 R. Veerasamy, T. Z. Xin, S. Gunasagaran, T. F. W. Xiang, E. F. C. Yang, N. Jeyakumar and S. A. Dhanaraj, *J. Saudi Chem. Soc.*, 2011, **15**, 113–120.
41 S. M. Ghoreishi, M. Behpour and M. Khayatkashani, *Phys. E*, 2011, **44**, 97–104.
42 A. K. Mittal, Y. Chisti and U. C. Banerjee, *Biotechnol. Adv.*, 2013, **31**, 346–356.
43 A. K. Jha, K. Prasad, V. Kumar and K. Prasad, *Biotechnol. Prog.*, 2009, **25**, 1476–1479.
44 N. Ahmad, S. Sharma, V. N. Singh, S. F. Shamsi, A. Fatma and B. R. Mehta, *Biotechnol. Res. Int.*, 2011, **2011**, 1–8.
45 S. Panigrahi, S. Kundu, K. Ghosh, S. Nath and T. Pal, *J. Nanopart. Res.*, 2004, **6**, 411–414.
46 L. Clem Gruen, *Biochim. Biophys. Acta*, 1975, **386**, 270–274.
47 Y. N. Tan, J. Y. Lee and D. I. C. Wang, *J. Am. Chem. Soc.*, 2010, **132**, 5677–5686.
48 S. Li, Y. Shen, A. Xie, X. Yu, L. Qiu, L. Zhang and Q. Zhang, *Green Chem.*, 2007, **9**, 852–885.
49 J. Huang, Q. Li, D. Sun, Y. Lu, Y. Su, X. Yang, H. Wang, Y. Wang, W. Shao, N. He, J. Hong and C. Chen, *Nanotechnology*, 2007, **18**, 105104–105115.

50 J. Kesharwani, K. Y. Yoon, J. Hwang and M. Rai, *J. Bionanosci.*, 2009, **3**, 39–44.
51 M. Shah, D. Fawcett, S. Sharma, S. K. Tripathy and G. E. J. Poinern, *Materials*, 2015, **8**, 7278–7308.
52 N. Shreyash, S. Bajpai, M. A. Khan, Y. Vijay, S. K. Tiwary and M. Sonker, *ACS Appl. Nano Mater.*, 2021, **4**, 11428–11457.
53 A. K. Mittal, J. Bhaumik, S. Kumar and U. C. Banerjee, *J. Colloid Interface Sci.*, 2014, **415**, 39–47.
54 J. Singh, T. Dutta, K. H. Kim, M. Rawat, P. Samddar and P. Kumar, *J. Nanobiotechnol.*, 2018, **16**, 84.
55 M. A. Azeez, F. A. Durodola, A. Lateef, T. A. Yekeen, A. O. Adubi, I. C. Oladipo, E. A. Adebayo, J. A. Badmus and A. O. Abawulem, in *IOP Conference Series: Materials Science and Engineering*, Institute of Physics Publishing, 2020, vol. 805.
56 M. Waseem and M. A. Nisar, in *Functionalized Nanomaterials*, InTech, 2016.
57 S. Ambika and M. Sundrarajan, *J. Photochem. Photobiol., B*, 2015, **146**, 52–57.
58 O. J. Nava, P. A. Luque, C. M. Gómez-Gutiérrez, A. R. Vilchis-Nestor, A. Castro-Beltrán, M. L. Mota-González and A. Olivas, *J. Mol. Struct.*, 2017, **1134**, 121–125.
59 M. Ovais, A. Raza, S. Naz, N. U. Islam, A. T. Khalil, S. Ali, M. A. Khan and Z. K. Shinwari, *Appl. Microbiol. Biotechnol.*, 2017, **101**, 3551–3565.
60 S. Kumar, G. Saeed, L. Zhu, K. N. Hui, N. H. Kim and J. H. Lee, *Chem. Eng. J.*, 2021, **403**, 126352.
61 A. Burke, *J. Power Sources*, 2000, **91**, 37–50.
62 J. Xie, P. Yang, Y. Wang, T. Qi, Y. Lei and C. M. Li, *J. Power Sources*, 2018, **401**, 213–223.
63 M. Dai, D. Zhao and X. Wu, *Chin. Chem. Lett.*, 2020, **31**, 2177–2188.
64 G. Zhang, X. Xiao, B. Li, P. Gu, H. Xue and H. Pang, *J. Mater. Chem. A*, 2017, **5**, 8155–8186.
65 D. Majumdar, *J. Electroanal. Chem.*, 2021, **880**, 114825.
66 A. González, E. Goikolea, J. A. Barrena and R. Mysyk, *Renewable Sustainable Energy Rev.*, 2016, **58**, 1189–1206.
67 B. Pal, S. Yang, S. Ramesh, V. Thangadurai and R. Jose, *Nanoscale Adv.*, 2019, **1**, 3807–3835.
68 Y. Gogotsi and R. M. Penner, *ACS Nano*, 2018, **12**, 2081–2083.
69 L. W. Le Fevre, J. Cao, I. A. Kinloch, A. J. Forsyth and R. A. W. Dryfe, *ChemistryOpen*, 2019, **8**, 418–428.
70 Y. Jiang and J. Liu, *Energy Environ. Mater.*, 2019, **2**, 30–37.
71 X. You, M. Misra, S. Gregori and A. K. Mohanty, *ACS Sustain. Chem. Eng.*, 2018, **6**, 318–324.
72 W. Zuo, R. Li, C. Zhou, Y. Li, J. Xia and J. Liu, *Adv. Sci.*, 2017, **4**, 1600539.
73 B. E. Conway, V. Birss and J. Wojtowicz, *J. Power Sources*, 1997, **66**, 1–14.
74 D. Majumdar and S. Ghosh, *J. Energy Storage*, 2021, **34**, 101995.
75 D. Majumdar, M. Mandal and S. K. Bhattacharya, *ChemElectroChem*, 2019, **6**, 1623–1648.
76 D. Majumdar, *ChemElectroChem*, 2021, **8**, 291–336.
77 D. Majumdar, T. Maiyalagan and Z. Jiang, *ChemElectroChem*, 2019, **6**, 4343–4372.
78 N. Chen, L. Ni, J. Zhou, G. Zhu, Y. Zhang, S. Chen, F. Gao, C. Lu, H. Ji, J. Chen, X. Wang, X. Guo, L. Peng, W. Ding and W. Hou, *Sustainable Energy Fuels*, 2018, **2**, 2788–2798.
79 M. Okubo, E. Hosono, J. Kim, M. Enomoto, N. Kojima, T. Kudo, H. Zhou and I. Honma, *J. Am. Chem. Soc.*, 2007, **129**, 7444–7452.
80 L. Kong, X. Liu, J. Wei, S. Wang, B. Bin Xu, D. Long and F. Chen, *Nanoscale*, 2018, **10**, 14165–14170.
81 C. Costentin and J. M. Savéant, *Chem. Sci.*, 2019, **10**, 5656–5666.
82 H. Huang and M. Niederberger, *Nanoscale*, 2019, **11**, 19225–19240.
83 H. S. Kim, J. B. Cook, H. Lin, J. S. Ko, S. H. Tolbert, V. Ozolins and B. Dunn, *Nat. Mater.*, 2017, **16**, 454–462.
84 L. Guan, L. Yu and G. Z. Chen, *Electrochim. Acta*, 2016, **206**, 464–478.
85 T. Brousse, D. Bélanger and J. W. Long, *J. Electrochem. Soc.*, 2015, **162**, A5185–A5189.
86 S. Najib and E. Erdem, *Nanoscale Adv.*, 2019, **1**, 2817–2827.
87 S. Huang, X. Zhu, S. Sarkar and Y. Zhao, *APL Mater.*, 2019, **7**, 100901.
88 B. Kay Hyeok An, W. Seok Kim, Y. Soo Park, Y. Chul Choi, S. Mi Lee, D. Chul Chung, D. Jae Bae, S. Chu Lim, Y. Hee Lee, Y. H. Lee, K. H. An, W. S. Kim, Y. S. Park, Y. C. Choi, S. M. Lee, D. J. Bae, S. C. Lim and D. C. Chung, *Adv. Mater.*, 2001, **13**, 497–500.
89 M. E. Plonska-Brzezinska and L. Echegoyen, *J. Mater. Chem. A*, 2013, **1**, 13703–13714.
90 Y. Gao, Y. S. Zhou, M. Qian, X. N. He, J. Redepenning, P. Goodman, H. M. Li, L. Jiang and Y. F. Lu, *Carbon N. Y.*, 2013, **51**, 52–58.
91 G. Zhang, X. Xiao, B. Li, P. Gu, H. Xue and H. Pang, *J. Mater. Chem. A*, 2017, **5**, 8155–8186.
92 P. Simon and Y. Gogotsi, *Nat. Mater.*, 2008, **7**, 845–854.
93 Y. N. Zhang, C. Y. Su, J. L. Chen, W. H. Huang and R. Lou, *Rare Metals*, 2023, **42**, 769–796.
94 Y. Qiao, J. He, Y. Zhou, S. Wu, X. Li, G. Jiang, G. Jiang, M. Demir and P. Ma, *ACS Appl. Mater. Interfaces*, 2023, **15**, 52381–52391.
95 C. Largeot, C. Portet, J. Chmiola, P.-L. Taberna, Y. Gogotsi and P. Simon, *J. Am. Chem. Soc.*, 2008, **130**, 2730–2731.
96 Y. Wang, J. Guo, T. Wang, J. Shao, D. Wang and Y. W. Yang, *Nanomaterials*, 2015, **5**, 1667–1689.
97 P. Simon and Y. Gogotsi, *Nat. Mater.*, 2020, **19**, 1151–1163.
98 J. Liu, Z. Xu, B. Zhu, X. Du, Y. Yang, C. Yi, Z. Zhang, C. Cai and J. Li, *RSC Adv.*, 2018, **8**, 19103–19115.
99 L. Wang and X. Hu, *Chem.–Asian J.*, 2018, **13**, 1518–1529.
100 Y. Ren, T. Zhu, Y. Liu, Q. Liu and Q. Yan, *Small*, 2021, **71**, 2008047.
101 I. L. Ikhioya, E. U. Onoh, A. C. Nkele, B. C. Abor, B. C. N. Obitte, M. Maaza and F. I. Ezema, *East Eur. J. Phys.*, 2023, **2023**, 162–172.
102 S. Ravichandran, J. Radhakrishnan, P. Sengodan and R. Rajendran, *J. Mater. Sci.: Mater. Electron.*, 2022, **33**, 9403–9411.
103 A. C. Nwanya, M. M. Ndipingwi, N. Mayedwaa, L. C. Razanamahandry, C. O. Ikpo, T. Waryo,

S. K. O. Ntwampe, E. Malenga, E. Fosso-Kankeu, F. I. Ezema, E. I. Iwuoha and M. Maaza, *Electrochim. Acta*, 2019, **301**, 436–448.
104 R. Teimuri-Mofrad, R. Hadi, H. Abbasi, E. Payami and S. Neshad, *J. Organomet. Chem.*, 2019, **899**, 120915.
105 Y. N. Sudhakar, H. Hemant, S. S. Nitinkumar, P. Poornesh and M. Selvakumar, *Ionics*, 2017, **23**, 1267–1276.
106 M. Xu, M. Sun, S. ur Rehman, K. Ge, X. Hu, H. Ding, J. Liu and H. Bi, *Chin. Chem. Lett.*, 2021, **32**, 2027–2032.
107 T. Wei, N. Zhang, Y. Ji, J. Zhang, Y. Zhu and T. Yi, *Chin. Chem. Lett.*, 2022, **33**, 714–729.
108 J. Meena, G. Pavithra, D. Anusha, A. S. Kumar and K. Santhakumar, *J. Mater. Sci.: Mater. Electron.*, 2023, **34**, 1131.
109 M. Saini, S. Yadav, N. Rani, A. Mushtaq, S. Rawat, K. Saini and D. Maity, *Mater. Sci. Eng., B*, 2023, **14**, 2304.
110 M. Shirzad Choubari, J. Mazloom and F. E. Ghodsi, *Ceram. Int.*, 2022, **48**, 21385–21395.
111 I. Shaheen, K. S. Ahmad, C. Zequine, R. K. Gupta, A. G. Thomas and M. A. Malik, *RSC Adv.*, 2021, **11**, 23374–23384.
112 I. Shaheen, K. S. Ahmad, C. Zequine, R. K. Gupta, A. G. Thomas and M. A. Malik, *New J. Chem.*, 2020, **44**, 18281–18292.
113 S. Chakraborty, M. Amalraj and N. L. Mary, *J. Energy Storage*, 2020, **28**, 101275.
114 T. N. Amirabad, A. A. Ensafi, K. Z. Mousaabadi, B. Rezaei and M. Demir, *Int. J. Hydrogen Energy*, 2023, **48**, 29471–29484.
115 B. Dinesh, N. Saravanan and A. S. Kumar, *Chem. Eng. J. Adv.*, 2022, **11**, 100311.
116 S. Nayak, A. A. Kittur and S. Nayak, *J. Electron. Mater.*, 2023, **52**, 1437–1447.
117 S. A. Al Kiey and M. S. Hasanin, *Environ. Sci. Pollut. Res.*, 2021, **28**, 66888–66900.
118 P. Lamba, P. Singh, P. Singh, A. Kumar, P. Singh, Bharti, Y. Kumar and M. Gupta, *Ionics*, 2021, **27**, 5263–5276.
119 L.-M. Wan, Q.-Y. Xia, J.-H. Wu, J. Liu, Z.-Y. Shi, S. Lan, T. Zhai, S. V Savilov, S. M. Aldoshin and H. Xia, *Rare Met.*, 2023, **42**, 39–46.
120 A. González, E. Goikolea, J. A. Barrena and R. Mysyk, *Renewable Sustainable Energy Rev.*, 2016, **58**, 1189–1206.
121 T. N. Vinuth Raj, P. A. Hoskeri, S. Hamzad, M. S. Anantha, C. M. Joseph, H. B. Muralidhara, K. Yogesh Kumar, F. A. Alharti, B. H. Jeon and M. S. Raghu, *Inorg. Chem. Commun.*, 2022, **142**, 109648.
122 N. Sobti, S. Chaguetmi, S. Achour, L. Chaperman, F. Mammeri and S. Ammar-Merah, *Solid State Sci.*, 2021, **113**, 106551.
123 M. Yassine and D. Fabris, *Energies*, 2017, **10**, 1340.
124 T. L. Soundarya, C. G Udayabhanu, Y. T. Ravikiran, B. Nirmala and G. Nagaraju, *J. Mater. Sci.: Mater. Electron.*, 2022, **33**, 10902–10918.
125 P. Naresh Kumar Reddy, D. P. M. D. Shaik, V. Ganesh, D. Nagamalleswari, K. Thyagarajan and P. Vishnu Prasanth, *Appl. Surf. Sci.*, 2021, **561**, 150092.
126 N. Kumar Reddy, P. Shaik, D. Nagamalleswari, D. Thyagarajan, V. Prasanth, N. Kumar Reddy, et al., *Indian J. Sci. Technol.*, 2021, **14**, 2766–2772.
127 A. Waris, H. Anwer, F. Abdulaziz, S. Latif, A. Alanazi, S. Sultana and M. Zain Khan, *Mater. Sci. Eng., B*, 2023, **291**, 116367.
128 Z. Xu, X. Zhang, K. Li, H. Lin, X. Qian and K. Sheng, *Energy Fuel*, 2021, **35**, 827–838.
129 B. Nisha, Y. Vidhyalakshmi and S. Abdul Razack, *Adv. Powder Technol.*, 2020, **31**, 1001–1006.
130 H. E. Nsude, K. U. Nsude, G. M. Whyte, R. M. Obodo, C. Iroegbu, M. Maaza and F. I. Ezema, *J. Nanopart. Res.*, 2020, DOI: **10.1007/s11051-020-05071-7**.
131 H. Bishwakarma, R. Tyagi, N. Kumar and A. K. Das, *Environ. Res.*, 2023, **218**, 115021.
132 S. Yadav, N. Rani and K. Saini, in *Materials Today: Proceedings*, Elsevier Ltd, 2021, vol. 49, pp. 2124–2130.
133 N. Rani, M. Saini, S. Yadav, K. Gupta, K. Saini and M. Khanuja, in *AIP Conference Proceedings*, American Institute of Physics Inc., 2020, vol. 2276.
134 S. Nayak, A. A. Kittur and S. Nayak, *Chem. Phys. Lett.*, 2022, **806**, 140058.
135 J. Uma, S. Banumathi, R. Maheswaran, N. Senthilkumar and B. Balraj, *J. Supercond. Nov. Magn.*, 2021, **34**, 817–823.
136 J. Kalaiarasi, C. Pragathiswaran and P. Subramani, *J. Mol. Struct.*, 2021, **1214**, 130704.
137 I. Shaheen, K. S. Ahmad, C. Zequine, M. R. Sulaiman, R. K. Gupta, A. G. Thomas and M. A. Malik, *J. Mater. Sci.: Mater. Electron.*, 2021, **32**, 8460–8474.
138 M. I. Pratheepa and M. Lawrence, *SN Appl. Sci.*, 2020, **2**, 318.
139 I. Shaheen, K. S. Ahmad, C. Zequine, R. K. Gupta, A. G. Thomas and M. A. Malik, *New J. Chem.*, 2020, **44**, 18281–18292.
140 V. Raja, G. Selvam, R. Anbarasu and S. Baskar, *Indian J. Sci. Technol.*, 2019, **12**, 107–108.
141 C. Sasirekha, S. Arumugam and G. Muralidharan, *Appl. Surf. Sci.*, 2018, **449**, 521–527.
142 A. M. Alturki, *Biomass Convers. Biorefin.*, 2022, DOI: **10.1007/s13399-022-03303-5**.
143 J. S. Kumar, M. Jana, P. Khanra, P. Samanta, H. Koo, N. C. Murmu and T. Kuila, *Electrochim. Acta*, 2016, **193**, 104–115.
144 M. Kundu, G. Karunakaran and D. Kuznetsov, *Powder Technol.*, 2017, **311**, 132–136.
145 E. Ismail, S. Khamlich, M. Dhlamini and M. Maaza, *RSC Adv.*, 2016, **6**, 86843–86850.
146 P. M. Anjana, M. R. Bindhu and R. B. Rakhi, *Mater. Sci. Energy Technol.*, 2019, **2**, 389–395.